BABEȘ - BOLYAI UNIVERSITY OF CLUJ - NAPOCA
FACULTY OF CHEMISTRY AND CHEMICAL ENGINEERING

A Kinetic Study on the Oxidation of Thiols and Mercaptoacids by several Transitional Metal Ions

Summary of Ph D. Thesis

Scientific Advisor
Prof. Dr. Ioan BÂLDEA

Ph.D Student
Dana-Maria SABOU

Cluj-Napoca
2011

BABEȘ - BOLYAI UNIVERSITY OF CLUJ - NAPOCA
FACULTY OF CHEMISTRY AND CHEMICAL ENGINEERING

A Kinetic Study on the Oxidation of Thiols and Mercaptoacids by several Transitional Metal Ions

Dana-Maria SABOU

Summary of Ph D. Thesis

Jury:

PRESIDENT
Assoc. Prof. Dr. Cornelia MAJDIK, Dean,
Faculty of Chemistry and Chemical Engineering, Babeş-Bolyai University, Cluj-Napoca

SCIENTIFIC ADVISOR
Prof. Dr. Ioan BÂLDEA, Babeş-Bolyai University, Cluj-Napoca

REVIEWERS
Prof. Dr. C. M. Rom. Acad. Dumitru OANCEA, University of Bucharest
Prof. Dr. Eng. Marcel Ionel POPA, Technical University "Gh. Asachi", Iaşi
Assoc. Prof. Dr. Eng. Alexandra Ana CSAVDARI, Babeş-Bolyai University, Cluj-Napoca

Cluj-Napoca
2011

CONTENTS OF THE THESIS

I. THEORETICAL CONSIDERATIONS ON REDOX PROCESSES

II. CHARACTERIZATION OF THE REACTING SYSTEMS INVESTIGATED IN THIS WORK

III. ORIGINAL CONTRIBUTIONS

A. OXIDATIONS OF THIOLACTIC ACID BY VARIOUS OXIDIZING SYSTEMS

B. OXIDATIONS OF OTHER THIOCOMPOUNDS BY CHROMIUM (VI)

Key Words: kinetics, homogeneous redox reactions, thiols, thiolactic acid, glutathione, benzyl mercaptan, transition metal ions, chromium VI, vanadium V, hexacyanoferrate III, spectrophotometry, ESR.

INTRODUCTION

One of the most prevalent classes of chemical processes, the oxidation-reduction (redox) reactions, contains the simplest of processes, such as the formation of a compound from its elements, as well as some of the most complex reactions, like those taking place in the living cells, either generating energy for them to live or governing their decay after death. Furthermore, oscillating reactions, taking place *in vitro* or *in vivo* also involve redox processes. It is therefore easily understood, that there is a great interest of scientists in this field to describe the intimate mechanisms of redox processes.

THE STRUCTURE OF THE PH.D THESIS

The Ph.D. thesis is made of two main sections. The first (Chapters I and II) gives a concise literature presentation of the class of redox reactions investigated (Chapter I) together with a description of the properties and reactions of the substances used in the kinetic study (Chapter II). The literature data focuses on the class of thiol compounds, with their anti-oxidizing character, in their reactions with various oxidants. The oxidizing character of Cr(VI), V(V), as well as that of Fe(III) in the hexacyanoferrate(III) complex, are described by several examples in order to provide a basis for the interpretations of the studies undertaken.

The second section (Chapter III) contains the personal contributions. It first provides a detailed presentation of the apparatuses and experimental procedures employed, and it continues by presenting the results obtained with the five reaction systems studied, as depicted in the scheme below.

Each system has been approached kinetically, searching for the involvement of some short-lived or long-lived intermediates to understand the details of their mechanism.

The general conclusions summarize the obtained results as well as the similarities or the difference occurring within these systems.

STUDIED SYSTEMS

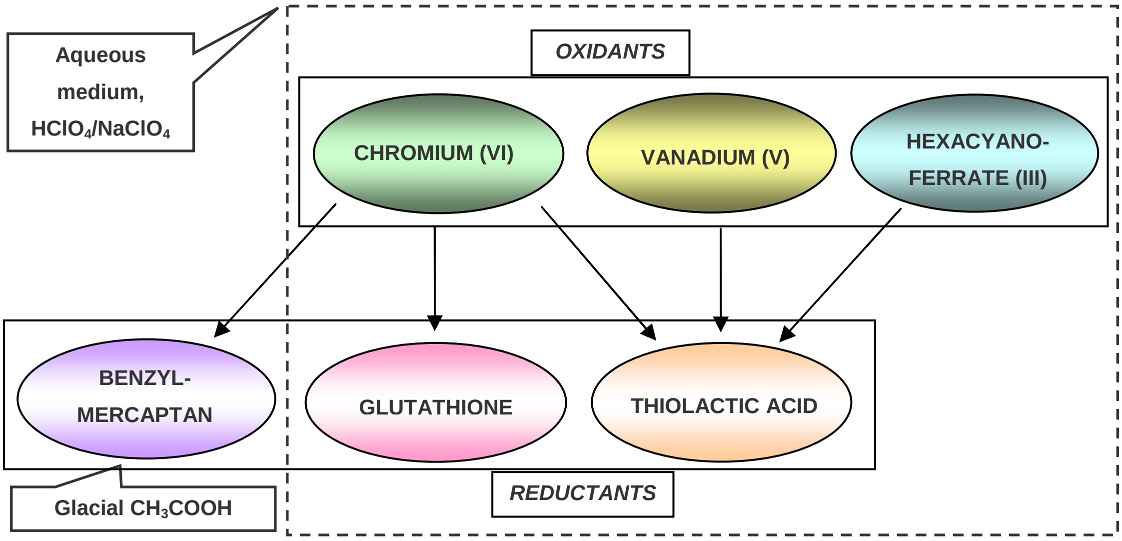

I. THEORETICAL CONSIDERATIONS ON REDOX PROCESSES

I.1. GENERAL ASPECTS

The most important feature of an oxidation-reduction reaction is the charge transfer between the participants. The electron transfer implies that changes must take place at the atomic level in the orbital populations of the two species, thus influencing the other bonds in which the respective atoms are involved.[1] This work approaches mixed redox reactions, taking as reducing agents several organic substrates and as oxidizing agents complexes of different transitional metals ion in their highest oxidation state.

I.2. THE ELECTRON-TRANSFER MECHANISM. OUTER-SPHERE AND INNER - SPHERE MECHANISMS.

Considering the electron transfer reaction and the structural changes accompanying it, Henry Taube[5] (Nobel prize 1983) classified these redox processes into two classes:

- outer-sphere redox processes
- inner-sphere redox processes.

Figure I.2.1 presents schematically the two ways of electron-transfer:

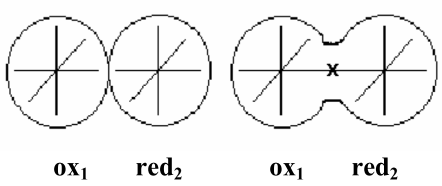

Figure I.2.1. Schematic representation of the interactions between reactants: outer-sphere (a) and inner-sphere (b)

Outer-sphere mechanisms involve a direct transfer between reducing and oxidizing agent with minimum of interaction. The coordination spheres do not suffer any modifications to their compositions, only some changes of ligand-metal ion distances and solvation interaction take place. The electron transfers by tunnelling and obeys the Franck-Condon restriction. The electron moves faster (10^{-15} s), while nuclei remain „frozen” in their actual positions, the time of their movement being much longer (10^{-13} s).

Taking into account the outer-sphere mechanism and self-exchange reactions (with no chemical transformation) Rudolph A. Marcus (Nobel prize 1992) introduced and developed a theoretical model to calculate rate constants for the electron-transfer[8,10]. Numerous inorganic reactions proved to obey this model[13-16]. The extention of this to organic reactions led to further elaboration of the theory by many other authors[18-21]. Some research has been done also on mixed inorganic-organic systems; a work to which we have contributed confirms the applicability of Marcus theory in the case of the oxidation of N,N,N',N'-tetramethyl-*p*-phenylendiammine (TMPPD) with $Fe(CN)_6^{3-}$, MnO_4^-, $Co(NH_3)_6^{3+}$and $Ru(OH)^{3+}$.[27]

Inner-sphere mechanisms, on the contrary, necessitate an intimate interaction between the coordination spheres of the reactants by linking them together in a complex having at least one ligand in common. This should precede the electron-transfer in a substitution process. The electron is transferred through this ligand having a role of a bridge. These mechanisms have three steps: a) formation of the complex with a common ligand as a bridge, b) electron-transfer c) dissociation of the complex into the reaction products[28]. Although, in principle, any of these steps might control the rate, in most situations the electron transfer occurs as the rate-determining step[1,2,29].

Transfer of the common ligand from the oxidizing species to the oxidized form of the reducing agent is a solid argument for the inner-sphere mechanism[37]. A modification of the rate by changing the ligand having the role of bridge is another support of such a mechanism. On the contrary, the lack of such influence argues for an outer-sphere mechanism.

Generally, systems which are inert to substitution will react by an outer-sphere pathway. For systems labile to substitution, a redox rate which is comparable to the substitution rate indicates an inner-sphere interaction. More information on the way the electron transfer takes place is brought about by the activation parameters. A small activation enthalpy supports an outer-sphere mechanism.

I.3. OXIDATION OR REDUCTION OF THE COORDINATED LIGAND

Numerous studies have been seen where the species oxidized by the metal ions is an organic or inorganic substrate, brought as ligand into the first coordination sphere.[40-43] The inner-sphere complex (ML, M = metal, L = ligand) so formed decomposes to give the redox products. Alternatively, ML may decay *via* a competing route. This second case implies considerably different structures for ML and the activated complex of the redox process.

The occurrence of ML species can be actually detected, or only implied by the experimental form of the rate law. Examples of ligand oxidation are found in reactions of various oxidants, such as Ce^{IV}, Fe^{III}, Mn^{III}, Co^{III}, V^{V}, Cr^{VI}, Ag^{II} or Cu^{II}.

Fewer cases are encountered where the ligand is reduced. Complexes with molecular oxygen or peroxocomplexes[44] can serve as examples.

I.4. EVIDENCE OF THE INVOLVEMENT OF AN INTERMEDIATE

When the rate law suggests the involvement of an intermediate, the most direct evidence in found in measurements of its physico-chemical properties. This approach requires the existence of an experimental technique for its detection. Often, it is necessary that the intermediate is formed in quite high concentration (comparable to those of the reactants in the case of a rapid pre-equilibrium). Depending on the life-time of the intermediate, the detection may use classical techniques or some arrangements designed for rapid reactions. Two techniques that were employed in our present studies are *spectrophotometry* and *ESR spectrometry.*[45,46]

Proof that no intermediate exists

With the large difference between electronic spectra (UV-VIS) of reactants and products, the successive recordings of spectra during the reaction can bring information on the involvement of intermediate. The appearance of isosbestic points is a proof there is a linear correlation[47,48] of the concentrations of the species, meaning that the reactant is transformed directly into the product and no intermediate is present. If is not the case, or this appears only within a short period at the beginning of the reaction, and the intersection position is changed, it indicates that some intermediate of significant concentration is formed

I.5. CATALYSIS IN REDOX REACTIONS

Catalysis by another redox couple

This phenomenon occurs when a redox couple can mediate uni-equivqlent or bi-equivalent electron transfer. An example is the oxidation of Cr(III) to Cr(VI) by $S_2O_8^{2-}$, which is catalyzed by Ag(I). The latter is able to form Ag(III) with the bi-equivalent peroxydisulfate. This, then forms Ag(II) in a reaction with Ag(I). Ag(II) will react uni-equivalently with Cr(III), or another intermediate species of Cr, to finally form Cr(VI).

Numerous oxidations of organic compounds are catalyzed by redox couples. Such examples are OsO_4 catalysis *via* the formation of double bridged intermediates[57-59] or Ce(IV) catalysis *via* Ce(III) intermediates[60].

The couple Cu^{2+}/Cu^{+} exerts a catalytic effect on many redox systems[54-56]. Cu(II) easily accepts an electron to form Cu^{+}, which is quite an unstable species in solution and is rapidly oxidized by any oxidizing agent. This way, the switch helps the progress of the main redox reaction. Sometimes, this intervention is undesirable because the copper ion is one of the most commonly occurring impurities in chemicals, and may cause irreproducible results, which in turn make the interpretation of kinetic data difficult.

II. CHARACTERIZATION OF REACTING SYSTEMS UNDERTAKEN IN THIS WORK

II.1. THIOLS

Thio-compounds are organic substances containing sulphur and are present in nature, especially in living organisms. The thiols – or mercaptans – have at least one -SH group bound to a carbon atom, similar to the hydroxyl group in alcohols.

The oxidation of thiols

Due to the similarity to the hydroxyl group, often the reactions of these two classes of organic compounds are compared. When oxidation is considered, there is no similarity. In the case of alcohols, the atom changing its oxidation state is the carbon atom containing hydroxyl group[65-70]. On the contrary, thiols are oxidized at the thiol group[73-81]. Moreover, hydroxyl containing compounds are bi-equivalent reducing agents whereas – at a mild oxidation – thiols are one-equivalent reducing agents.

The oxidation of thiols takes place depending on the reaction conditions and the nature of oxidizing agent. The possible oxidation states are presented in figure II.1.2.

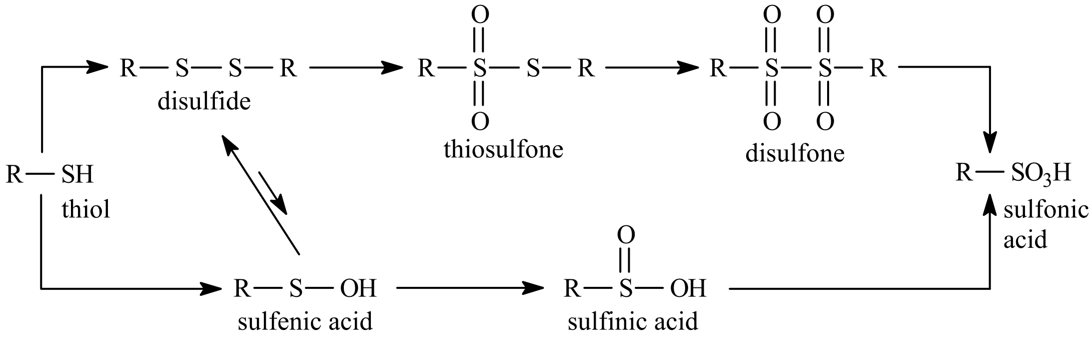

Figure II.1.2. Thio-compounds in various oxidation steps.

With strong oxidants, the very stable sulfonic acids are the ultimate species.

In the case of mild oxidation disulfides or sulfenic acids are the reaction products. Sulfenic acids are instable compounds and are oxidized further. Disulfides are quite stable, and, as a rule, are the final products under mild oxidation. They are formed by combination of thiyl radicals ($RS^{\bullet}$), through cleaving of the S–H bond. The disulfide formation can be bypassed if a more rapid reaction can take place. The free radicals pathway is the most frequently encountered paths to yield disulfide.

The studied thio-compounds

The structures of the three compounds investigated in this work, all are presented in figure II.1.3. All three of them are mono-thiols, but with otherwise quite different structures, which expectedly should reflect in their properties.

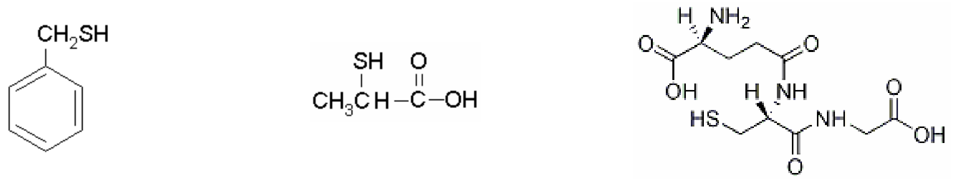

a. benzylmercaptan (α-toluene thiol) ***b.*** thiolactic acid (2-mercaptopropionic acid) ***c.*** glutathione (γ-glutamilcysteinylglycine)

Figura II.1.3. Structural formulas of the used thiols.

II.2. CHROMIUM (VI)

Like any other transitional metal, chromium displays multiple oxidation states. In aqueous solutions, the possible oxidation states are +6, +5, +4, +3 and +2. The +2 state is unstable and aggressively reducing. The +6 state, the highest for chromium, gives solutions with oxidizing properties. The unstable states +5 and +4 are also oxidizing by nature. The +3 state, in turn, is particularly stable for chromium, in air and aqueous solutions (acidic mostly) unlike for the other elements of its group. This makes Cr(III) both the product of Cr(II) oxidation and of Cr(VI) reduction, the latter taking place often in more steps, through formation of Cr(V) and/or Cr(IV).

Whatever the oxidation state, chromium forms coordinative complexes in aqueous solutions. Cr(III) has very good complexating properties; its complexes are hexa-coordinated, with octahedral geometry, the only generally inert to substitution chromium complexes. Those of Cr(II) are fewer, usually hexa-coordinated as well, weak and very labile to substitution; the replacement of the water ligand in the corresponding hexahydrate has rates close to the diffusion limit.[100] Cr(VI) is known to form tetrahedral anionic species, labile to substitution, which is why it reacts by inner sphere mechanisms. The instability of the electronic configurations of Cr(V) and Cr(IV) introduces some difficulties in studying their properties in general. Their complexes are also labile to substitution. For a long time those of Cr(V) were considered to be exclusively tetra-coordinated[65] and those of Cr(IV) hexa-coordinated, justifying in this way that the rate determining role was usually attributed to the formation of a Cr(IV) state in multi-step mechanisms, as this is requiring the most structural changes. More recent studies, many by ESR spectroscopy, have brought proof of penta- of even hexa-coordinated structures of some Cr(V) complexes[140,155,302b]. Some penta-coordinated[102] or even hepta-coordinated[104b] complexes of Cr(IV) with chelating ligands have also been prepared, thus opening the possibility for new structural interpretations of the species in solutions too[102a,105d].

Equilibria in Cr(VI) solutions

Depending on the acidity and total chromium concentration, various species can be found in aqueous solution, interconnected by equilibria[99,108], the main of which are listed below (eqs. 2.2.3.-2.2.7)

$$\mathrm{CrO_4^{2-} + H^+ \rightleftharpoons HCrO_4^-} \qquad \mathrm{K:}\ 7.94\cdot10^{5}\ (\mathrm{M^{-1}}) \tag{2.2.3}$$

$$\mathrm{HCrO_4^- + H^+ \rightleftharpoons H_2CrO_4} \qquad \mathrm{K:}\ 5.5\cdot10^{-1}\ (\mathrm{M^{-1}}) \tag{2.2.4}$$

$$\mathrm{2\,HCrO_4^- \rightleftharpoons Cr_2O_7^{2-} + H_2O} \qquad \mathrm{K:}\ \approx\ 158\ (\text{or } 98)^{109}\ (\mathrm{M^{-1}}) \tag{2.2.5}$$

$$\mathrm{Cr_2O_7^{2-} + H^+ \rightleftharpoons HCr_2O_7^-} \qquad \mathrm{K:}\ 1.41\cdot10^{-1}\ (\mathrm{M^{-1}}) \tag{2.2.6}$$

$$\mathrm{HCr_2O_7^- + H^+ \rightleftharpoons H_2Cr_2O_7} \qquad \mathrm{K:}\ \text{very small} \tag{2.2.7}$$

Computations based on these have rendered $HCrO_4^-$ as the major species in weak acidic solutions (pH 1÷5) of chromium concentration lower than 10^{-4} M [48].

Following the model of reaction 2.2.5, similar condensation processes involve species able to provide hydrogen ions[108,109,110b] (eq. 2.2.8).

$$\mathrm{HCrO_4^- + H^+ + X^- \rightleftharpoons XCrO_3^- + H_2O} \tag{2.2.8}$$

Such species could be acids used as medium for the reaction or the substrate itself. It often means that a first condensation with the acid in the medium takes place, creating a new species, which in turn will act as the oxidant for the substrate. The reactivity of the new form of the oxidant may vary appreciably from that of the $HCrO_4^-$. Perchloric acid in diluted solutions is considered amongst the most inert acids to such condensation, the reason for it being chosen as medium for many reactions, including those approached in this work.

Oxidations with chromium(VI)

Mechanistically, Cr(VI) oxidations proceed by inner-sphere. With an appropriate partner, the first step is an equilibrium of the type in 2.2.8[56,67,69,76,111,115,156,176-181]. The condensation complex formed further decomposes by transfer of electron(s). Most times, the redox step is rate determining. Cr(VI) accepts a total of three electrons in order to reduce to

Cr(III), that can transfer simultaneously or through various combinations of steps, passing through one or another unstable oxidation states. Such possibilities are illustrated in figure II.2.3.

The three-electron transfers are rare (one example is the reaction with sulphite ion); amongst the organic substrates they indicate co-oxidations[144], since no functional groups are able to provide all three electrons.

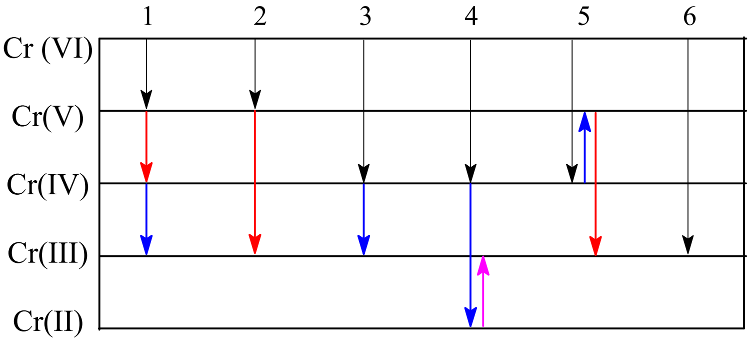

Figura II.2.3. Possible reaction routes for the reduction of Cr(VI)

The path of choice is the result of a compromise between the tendency of chromium to accept two electrons simultaneously and the substrate capacity of providing these electrons. When the tendencies match, as is the case for hydroxy-compounds, the bi-electronic route with Cr(IV) formation will be chosen. With thiols, on the other hand, that are one-electron reducing agents, the route *via* Cr(V) becomes of comparable importance[176-181]. Often, the two routes coexist. Once formed, the Cr(V) or Cr(IV) intermediates open new reaction paths for the substrate oxidation. These allude to the substantial complexity of oxidations by chromium(VI).

II.3. VANADIUM (V)

The chemistry of aqueous solutions of vanadium(V)[185,186]

The many species of vanadium (V) involved in just as many equilibria in aqueous solutions, are illustrated, but not exhausted, in the figure below. As can be seen, depending on the total vanadium concentration and on pH, the species acting as oxidant for a given substrate may vary significantly.

Also, factors such as temperature or ionic strength may affect the equilibria. This makes kinetic studies difficult, if only, from the perspective that one could hardly find a large enough range of conditions – a condition for a reliable kinetic study – over which to extend the study and at the same time, with reasonable approximation, deal with the same oxidant.

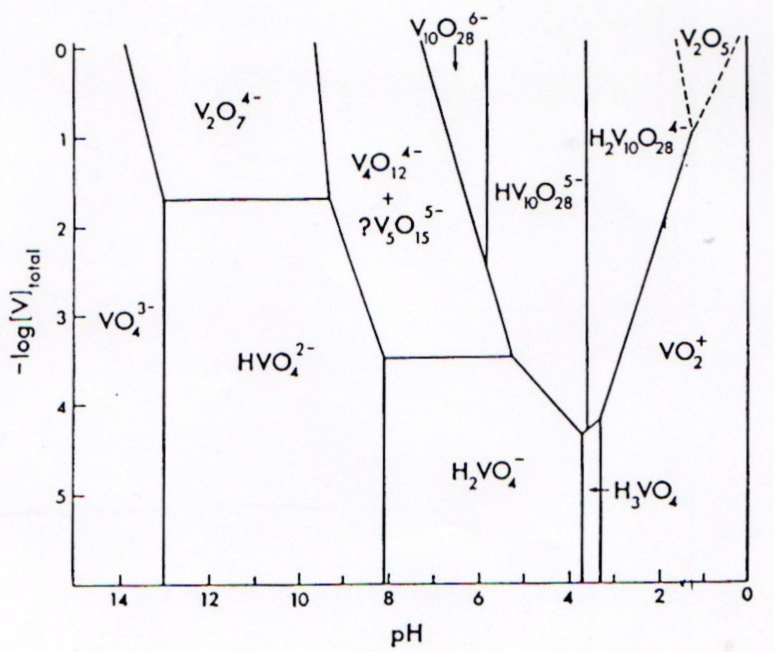

Figure II.3.1. Vanadium (V) species in aqueous solutions, as function of total vanadium concentration and pH of solution[186].

Oxidations by vanadium (V) of organic substances

Some of the features generally accepted[217] for the oxidations of organic substrates with vanadium (V), in the form VO_2^+, in acidic aqueous media, are inner-sphere mechanisms, mostly *via* 1:1 (sometimes also 1:2 or 2:1) V(V):substrate complex intermediates, and vanadium (IV) as a product. Still, bi-electronic reductions of V(V) to V(III) are often presumed, but further re-oxidation of V(III) is assumed, at the expense of another V(V). This is, nevertheless, more difficult to support when the reducing substrate is taken in excess.

With the decavanadate ion ($HV_{10}O_{28}^{5+}$), it was proposed that one unit at a time is displaced and reduced, rate determining being the fragmentation of the polyvanadate unit[214,215].

Lately, vanadium is studied in connection with biological thio-compounds, such as glutathione[218,219]. Attention is paid to the quite stable V(IV) complexes resulting from V(V) reduction by such thiols. Since V(IV) is isoelectronic with Cr(V), some structural similarities of their complexes is assumed, thus allowing the gain of further insight on the carcinogenic Cr(V) structure and behaviour.

II.4. HEXACYANOFERRATE (III)

Ferri- and ferro-cyanic complexes

Of the many oxidation states possible for iron, only the very usual +2 and +3 states form hexacyanoferric complexes, extremely stable species, inert to ligand substitution.
The hexacyanoferrate (III) ion ($Fe^{III}(CN)_6^{3-}$) also known as ferricyanide, is the completely de-protonated anion of ferricyanic acid ($H_3Fe(CN)_6$), a strong acid in all its dissociation steps[221].

$$H_3Fe(CN)_6 \rightleftharpoons H_2[Fe(CN)_6]^- + H^+ \qquad K_1 = 1{,}78\cdot 10^6\ M \tag{2.4.1}$$

$$H_2[Fe(CN)_6]^- \rightleftharpoons H[Fe(CN)_6]^{2-} + H^+ \qquad K_2 = 1{,}70\cdot 10^3\ M \tag{2.4.2}$$

$$H[Fe(CN)_6]^{2-} \rightleftharpoons Fe(CN)_6^{3-} + H^+ \qquad K_3 = 3{,}98\ M \tag{2.4.3}$$

Thus, on a large pH range, the completely dissociated form is the only one present in solution.

Similarly, hexacyanoferrate (II) ion ($Fe^{II}(CN)_6^{4-}$) also known as ferrocyanide, is the completely de-protonated form of the ferrocyanic acid ($H_4Fe(CN)_6$), which is also strong in its first and second dissociation steps, but weaker in its last two[227]:

$$H_4Fe(CN)_6 \rightleftharpoons H_3[Fe(CN)_6]^- + H^+ \qquad K_1' = 3{,}47\cdot 10^2\ M \tag{2.4.4}$$

$$H_3[Fe(CN)_6]^- \rightleftharpoons H_2[Fe(CN)_6]^{2-} + H^+ \qquad K_2' = 1{,}20\ \ M \tag{2.4.5}$$

$$H_2[Fe(CN)_6]^{2-} \rightleftharpoons H[Fe(CN)_6]^{3-} + H^+ \qquad K_3' = 2{,}24\cdot 10^{-3}\ M \tag{2.4.6}$$

$$H[Fe(CN)_6]^{3-} \rightleftharpoons Fe(CN)_6^{4-} + H^+ \qquad K_4' = 6{,}46\cdot 10^{-5}\ M \tag{2.4.7}$$

Therefore, $Fe(CN)_6^{4-}$ is protonated easier than $Fe(CN)_6^{3-}$ in media of the same acidity.

Oxidations with hexacyanoferrate (III)

Since the electron transfer in the hexacyanoferrate complexes takes place between the metallic centres, *the redox couple $[Fe(CN)_6]^{3-}/[Fe(CN)_6]^{4-}$* is a monoelectronic system. It is also very stable, due to the fact that both complex ions are inert to ligand substitution. That, in turn, means that almost without exception the oxidations with hexacyanoferrate(III) proceed by outer-sphere mechanisms[225]. A rate constant of $5{,}54\cdot 10^4\ M^{-1}s^{-1}$ has been determined for the electron transfer.

$$Fe(CN)_6^{3-} + e^- \rightleftharpoons Fe(CN)_6^{4-} \tag{2.4.11}$$

On the other hand, since H^+ ions are not involved in the redox equation, the standard potential of the couple is independent on acidity[233,234] over a large pH range (4÷13). Its relatively small value (0,41 V for $[K^+]$=0,1 M), makes hexacyanoferrate a weak oxidant. It acts, therefore, as a selective oxidizing agent, only appropriate for substrates highly susceptible to oxidation. Also, for substrates with more possible oxidation steps, it will be a mild oxidant, generally leading to the first such step.

The key step in any of its redox processes is the electron transfer. For this to take place, an ion pair, oxidant-substrate, intermediate is formed in a rapid pre-equilibrium. The electron transfer – and rate determining step – takes place inside the outer-sphere type precursor. The reaction orders with both the oxidant and the reducing agent are usually one.

The oxidations by hexacyanoferrate (III) are expected to be quite simple and “clean” of secondary processes due to their outer-sphere mechanisms, thus recommending it as oxidant. One limitation is the sensitivity to catalysis by trace ionic impurities, especially copper, brought in with the chemicals. This aspect needs to be either quantified, eliminated or at least minimized by using highly pure chemicals, if possible also from the same batch.

III ORIGINAL CONTRIBUTIONS

III.1. EXPERIMENTAL ASPECTS

In the large majority of the kinetic experiments of the thesis, the detection method was spectrophotometry in the ultra violet and visible (UV-VIS) range. Additionally, a series of experiments were conducted using electron spin resonance (ESR) spectroscopy.

In order to study processes of different time scales, different experimental setups were applied, including static or flow methods, with the latter used both in the stopped and continuous modes.

This chapter of the thesis describes the used apparatuses and the corresponding methods of operation. Further, the experimentally obtained data is presented and analyzed.

III.2. THE OXIDATION OF THIOLACTIC ACID BY Cr(VI) IN ACIDIC MEDIA[298]

Taking into account the equilibria involving Cr(VI)[99] species it is possible to chose conditions of its concentration and acidity to have the $HCrO_4^-$ species dominant in the solution. UV-VIS spectral measurements established these conditions.

Introductory aspects

Preliminary observations

A rapid change of solution color, from yellow to red-brown, taking place during the mixing of the two reactants acidic solutions, was seen, which pales as time elapses. This suggests the formation of an intermediate species during the reaction process.

Stoichiometry

The spectrophotometric titration, where the remaining Cr(VI) color was measured after the reaction has been accomplished in mixtures having increasing thiolactic acid (RSH) to Cr(VI) molar ratios, showed almost zero absorbance at ratios greater than 3. At lower ratios, the dependence showed no linear behavior because further oxidation to oxygenated products might take place (Fig. III.2.2.). This is in agreement with other literature data[115,172,173,176,177,179,299]

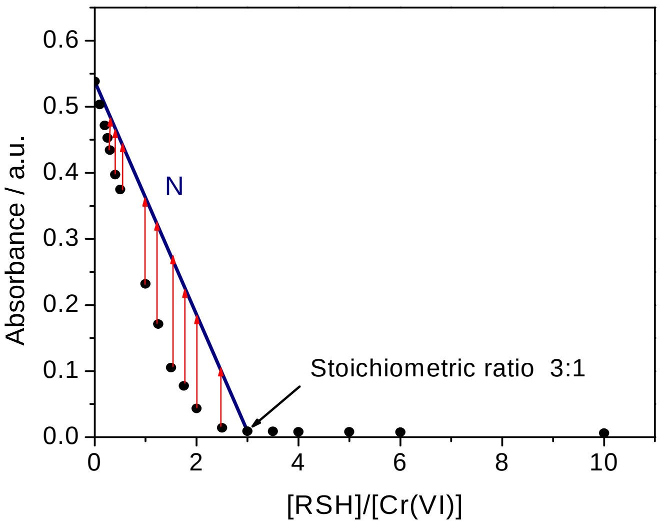

Figure III.2.2. Results of spectrophotometric titration. ([RSH] increasing, $[Cr(VI)]_0 = 6.67\cdot10^{-5}$ M, $[H^+] = 1\cdot10^{-3}$ M ($HClO_4$), $\mu = 0.5$ M ($NaClO_4$), T = 293 K)

To verify the 3 to 1 ratio, six reaction mixtures were allowed to complete the process and then the excess thiol was titrated iodometrically. The mean of these experiments showed a ratio of 3.09 ± 0.03 moles of thiolactic acid to react with 1 mole of Cr(VI). Therefore the overall stoichiometry is (where the coordination shell of Cr(III) complex is not specified):

$$6\ CH_3CH(COOH)SH + 2\ HCr^{VI}O_4^- + 8\ H^+ \longrightarrow 3\ (CH_3CH(COOH)S)_2 + 2\ Cr^{III} + 8\ H_2O \qquad 3.2.1$$

Electronic spectra. Evidence of an intermediate.

Electronic spectra of $HCrO4^-$, thiolactic acid and a reaction mixture at various time intervals are presented in figure III.2.3. It is observed that the mixture exhibits an absorption band around 420 nm. The batochromic shift of the charge-transfer maximum from 350 in $HCrO4^-$ to 420 nm in the mixture argues the change of an oxygen ligand of Cr(VI) with a sulphur, and a condensed compound of esteric type, thiolato-chromate, is formed. This takes place as shown in the following equilibria:

$$CH_3CH(COOH)SH + HOCrO_3^- \rightleftharpoons CH_3CH(COOH)SCrO_3^- + H_2O \qquad 3.2.2$$

$$CH_3CH(COOH)S^- + HOCrO_3^- + H^+ \rightleftharpoons CH_3CH(COOH)SCrO_3^- + H_3O^+ \qquad 3.2.3$$

The progress of the reaction can be followed at either 350 nm or 420 nm, yet neither of these wavelengths corresponds to a single species.

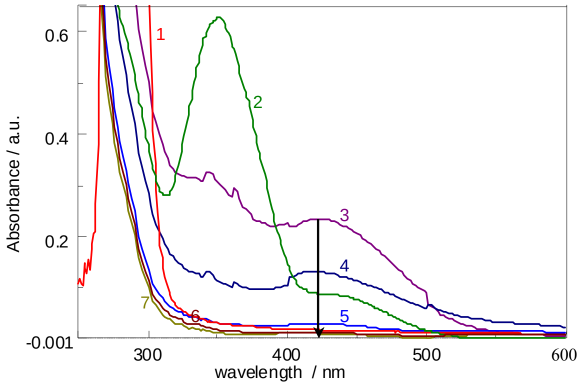

Figure III.2.3. Comparative spectra of the reactants and reaction mixture.
1- [RSH] = 0.1 M; **2**- [Cr(VI)]=$7.22 \cdot 10^{-5}$ M; **3**÷**7**- reaction mixtures at some time intervals
([RSH] = $2.67 \cdot 10^{-3}$ M, $[Cr(VI)]_0$ = $6.67 \cdot 10^{-5}$ M, $[H^+] = 3.16 \cdot 10^{-3}$ M, μ =0.5 M, T = 293 K)

REACTION KINETICS

Experimental curves. Mechanistic model and mathematic approach

The reaction is quite rapid and reaches accomplishment within several minutes. Figure III.2.4 presents examples of the absorbance evolution during time.

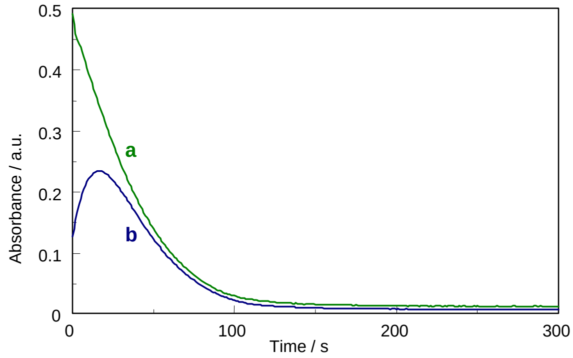

Figure III.2.4. (1) Experimental kinetic curves recorded at 350 nm and 420 mn **a**) 350 nm, **b**) 420 nm
([RSH] = $1.33 \cdot 10^{-3}$ M, $[Cr(VI)]_0$ = $6.67 \cdot 10^{-5}$ M, $[H^+] = 3.16 \cdot 10^{-2}$ M, μ =0.5 M, T = 293K.

The shape of the kinetic curve at 420 nm is a bi-phasic one, showing the presence of two consecutive processes. Both the recordings at 350 nm and at 420 nm seem to follow an exponential dependence, towards the end of the process. So, the mathematic model of the system is given as:

$$R + S\ (+\ H^+) \rightleftharpoons I\ (+\ H^+) \qquad k_1,\ k_{-1} \qquad 3.2.4$$

$$I\ (+\ S)\ (+\ H^+) \longrightarrow P\ (+\ H^+) \qquad k_2 \qquad 3.2.5$$

Under the excess concentration of substrate S, and also of that of hydrogen ion, which may intervene in the process as catalyst, this simplifies greatly, to:

$$R \xrightarrow{k_{1obs}} I \xrightarrow{k_{2obs}} P \qquad 3.2.6$$

That is a sequence of two apparent first order reactions, which can easily be manipulated. The integrated form of the absorbance evolution is:

$$A - A_{\infty} = [R]_0 \ell \{e_R + \frac{k_{2obs}\varepsilon_P - k_{1obs}\varepsilon_I}{k_{1obs} - k_{2obs}}\} e^{-k_{1obs}t} + [R]_0 \ell \{\frac{k_{1obs}(\varepsilon_I - \varepsilon_P)}{k_{1obs} - k_{2obs}}\} e^{-k_{2obs}t} \qquad 3.2.8$$

where A and A_{∞} stand for actual and final absorbances, ℓ is the path length of the cell and ε_R, ε_I, and ε_P are the molar absorptivities of reactant R, intermediate I, and product P. A simpler form (by grouping, next to an exponential term, all constants in one) can be obtained:

$$A - A_{\infty} = \gamma_1 e^{-k_{1obs}t} + \gamma_2 e^{-k_{2obs}t} \qquad 3.2.9$$

Data processing: *Method A – linear regression.* A classical approach of manipulation of this equation in order to obtain rate constants is linearization. When the condition $k_{1obs} > 5\ k_{2obs}$ is fulfilled[300], at long times of the reaction, the first exponential term vanishes (only the second step proceeds) and it is possible to determine k_{2obs} and γ_2 from a linear logarithmic form.

$$A - A_{\infty} = \gamma_2 e^{-k_{2obs}t} \qquad 3.2.10$$

For the beginning of the process, where the formation of intermediate prevails, another equation can be derived:

$$\ln(A - A_{\infty}) = \ln \gamma_2 - k_{2obs}t \qquad 3.2.11$$

which in its linear form permits the determination of γ_1 and k_{1obs}.

$$\ln\left(A - A_{\infty} - \gamma_2 e^{-k_{2obs}t}\right) = \ln \gamma_1 - k_{1obs}t \qquad 3.2.13$$

The handling of data has been done using Microsoft Excel, where simple linear regressions were performed. At long times (after more than 90 % of reaction) the behavior is linear with R^2 between 0.9925 and 0.9990. The plots of equation 3.2.13 were also linear ($R^2 \in [0.9911 \div 0.9999]$) at short time after mixing. Experimental kinetic curves at 350 nm and 420 nm led to comparable values, as shown in table III.2.1.

Some advantages and limitations of this method are discussed in detail in the thesis, commenting on the selection of the time range to be employed for the curves to compute the rate coefficients, as well as on the condition $k_{1obs} > 5\ k_{2obs}$ which is not fulfilled.

Table III.2.1. Mean values (3-5 individual runs) of k_{2obs} and k_{1obs} obtained under similar conditions at the two λ ($[HCrO_4^-] = 6.67 \times 10^{-5}$ M, T = 293 K, μ = 0.5 M).

$10^3 \cdot$[RSH] (M)	$10^2 \cdot [H^+]$ (M)	$k_{2obs, med}$ (s^{-1})		$k_{1obs, med}$ (s^{-1})		$k_{1obs, med}$ / $k_{2obs, med}$		k_{420} / k_{350}	
		350 nm	**420 nm**	**350 nm**	**420 nm**	**350 nm**	**420 nm**	$k_{2obs, med}$	$k_{1obs, med}$
3.3	7.93	0.108	0.117	0.21	0.25	1.94	2.14	1.08	1.19
3.3	6.24	0.100	0.107	0.19	0.22	1.90	2.06	1.07	1.16
3.3	1.97	0.075	0.077	0.100	0.120	1.33	1.56	1.03	1.20
3.3	0.79	0.061	0.062	0.080	0.090	1.31	1.45	1.02	1.13
3.3	0.65	0.060	0.062	0.078	0.087	1.30	1.40	1.03	1.12
3.3	3.12	0.086	0.077	0.136	0.135	1.58	1.75	0.90	0.99
1.3	3.12	0.038	0.035	0.048	0.053	1.26	1.51	0.92	1.10
4.0	3.12	0.100	0.091	0.16	0.16	1.64	1.80	0.91	1.00
5.3	3.12	0.134	0.117	0.21	0.21	1.60	1.75	0.87	0.96
6.7	3.12	0.150	0.139	0.24	0.24	1.61	1.76	0.93	1.01

Obs. Estimated standard errors of the means are around 5% for k_{2obs} and 5-6% for k_{1obs}, if taking into account the propagation of errors for the individual runs, but, for $k_{1obs,}$ not taking into account the errors due to k_{2obs} and γ_2.

Data processing: *Method B – non-linear regression.* The un-manipulated experimental curves were fitted with an equation which has a kinetic meaning, derived from the supposed mathematical model. For this, equation 3.2.9 was written in the form below, which satisfies the requirements of the software used.

$$Y = F_1 \cdot e^{(-k_{1obs}(X+X_0))} + F_2 \cdot e^{(-k_{2obs}(X+X_0))} + Y_0 \qquad 3.2.14$$

with $F_1 = 0.0003335 \cdot (\varepsilon_R - \frac{\varepsilon_I \cdot k_{1obs}}{k_{1obs} - k_{2obs}} + \frac{\varepsilon_P \cdot k_{2obs}}{k_{1obs} - k_{2obs}})$ and $F_2 = 0.0003335 \cdot k_{1obs}(\frac{\varepsilon_I - \varepsilon_P}{k_{1obs} - k_{2obs}})$

and where $Y = A$ (absorbance), $X = t$ (time), X_0 = time delay at the start of data acquisition, Y_0 = a correction factor for base line (the translation of the curve along the Y axis, including A_∞), $0.0003335 = [Cr(VI)]_0 \cdot \ell$, and k_{1obs}, k_{2obs}, ε_R, ε_I and ε_P all are as described above.

B1. Fitting single curves. The program TableCurve 2D 5.0 (Systat Software) has been used. It operates by successive iterations varying the specified parameters in order to get the best fit. Details of the initialization and the limitations are given in the thesis along with molar absorbance coefficients and time delays. The results seem to be comparable to those of method A, although method A appears to overestimate k_{1obs}.

B2. Fitting groups of curves. The program Origin 8.0 (Origin Labs) has been employed for fitting groups of individual runs using a nonlinear least squares method (Levenberg-Marquardt). In these fits, certain parameters were required to be identical for all curves, thus imposing global conditions on the fit. For example, in a set where the concentration of one species was varied, and those of the other reactants together with the rest of the experimental conditions were kept the same, the restraint that the value of the molar absorptivity of the intermediate should be identical for all curves in the group, was used. Figure III.2.6 presents a comparison of the fits and experimental points, showing a very good superposition, particularly when the contribution of the end-part of the reaction to the curve has been "equilibrated" by removing of the excess readings (points) in this region.

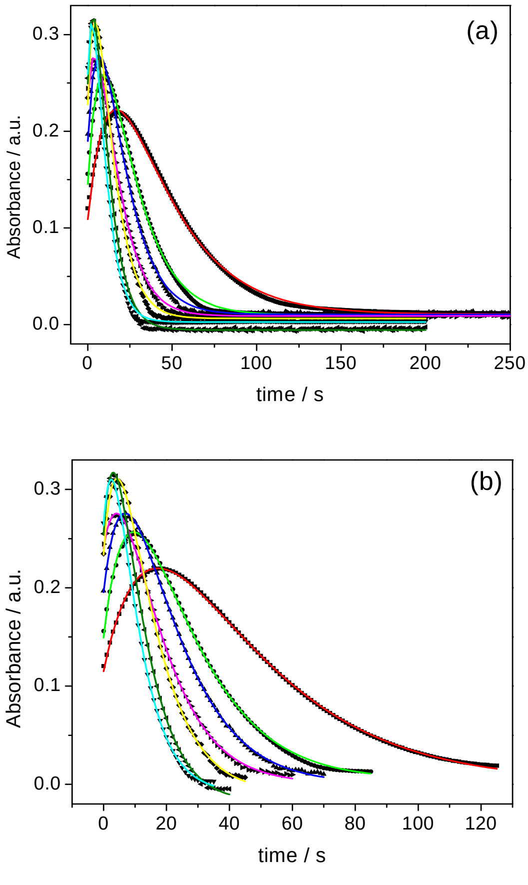

Figure III.2.6. "Global" fits by Origin 8.0 of a selection of curves by using all the points (a), or by elimination the final tail (b) (T=293K, μ.=0.5 M, [H^+] = 0.0316 M; [RSH]= variable).

A comparison of the three methods of handling the data is presented in table III.2.5. There are some differences between the methods, but the errors are of the same order of magnitude between the two variants of fitting. The somewhat smaller errors of the method B2 are the result of the statistic n greatly enhanced by the use of the points of more curves. The two fitting methods have the advantage that, by determining k_{1obs} and k_{2obs} simultaneously, both of them rely on each other's precision, thus improving mostly the results on k_{1obs}.

Tabel III.2.5. Comparison of the mean values of k_{1obs} and k_{2obs} and their estimated errors (%), obtained by the three different methods (T = 293 K, $[H^+]_0=3.12\cdot10^{-2}$ M, $[Cr(VI)]_0=6.67\cdot10^{-5}$ M)

10^3 [RSH] (M)	Method A				Method B1		Method B2	
	350 nm		420 nm		420 nm		420nm	
	k_{1obs} (s^{-1})	*rel. error (%)	k_{1obs} (s^{-1})	*rel. error (%)	k_{1obs} (s^{-1})	rel. error (%)	k_{1obs} (s^{-1})	rel. error (%)
1.3	0.048	10.9	0.053	12.3	0.051	7.8	0.038	3.2
2.7	0.120	4.3	0.110	4.5	0.086	6.8	0.071	3.5
3.3	0.136	5.6	0.135	5.7	0.104	6.3	0.092	3.8
4.0	0.164	4.4	0.164	6.5	0.130	6.9	0.113	4.1
5.3	0.213	4.8	0.205	4.9	0.182	7.3	0.163	4.8
6.7	0.241	5.7	0.244	6.9	0.216	6.5	0.202	5.1
8.0	-	-	0.297	7.5	0.253	6.1	0.224	5.1
	k_{2obs} (s^{-1})	rel. error (%)	k_{2obs} (s^{-1})	rel. error (%)	k_{2obs} (s^{-1})	rel. error (%)	k_{2obs} (s^{-1})	rel. error (%)
1.3	0.039	3.8	0.035	6.2	0.048	7.2	0.055	3.2
2.7	0.081	4.3	0.063	3.5	0.066	7.2	0.081	3.6
3.3	0.087	4.3	0.077	3.7	0.087	5.9	0.089	3.8
4.0	0.100	3.7	0.091	4.7	0.101	6.7	0.100	3.9
5.3	0.136	6.9	0.117	5.3	0.129	5.4	0.111	4.4
6.7	0.150	4.8	0.139	5.0	0.148	4.0	0.130	4.4
8.0	-	-	0.150	5.4	0.177	4.8	0.149	4.2

* The errors of these rate coefficients do not contain the errors due to individual k_{2obs} determination. With those, there should be less significant digits to some values (as given in other tables); the extra digit was here kept solely for comparison purpose.

Although the values of the rate constants differ sometimes, the handling in the kinetic interpretation leads to the same conclusions. Taking into consideration that there are fewer restrictions with the method B1, it was chosen to present the data obtained this way.

Thus far it has been established that the process takes place by two distinct steps, the first being the formation of a condensed intermediate that reacts further towards the products. The apparent rate constants for the two processes are functions of the reaction conditions (concentration, acidity, temperature and ionic strength).

Kinetics of the intermediate formation

As the concentration of organic substrate and acidity are in large excess, the rate coefficient dimensions (s^{-1}) correspond to first order in $HCrO_4^-$, which is the limiting reactant. To find the reaction order of the excess reactants, the model implies that k_{1obs} can be written as $k_{1obs} = k_1[RSH]_0^a[H^+]_0^b + k_{-1}[H^+]^b$, taking into account both directions of the equilibrium.

Under thiolactic acid excess, the first term prevails. Making use of log – log plots, the equation is

$$\lg k_{1obs} = \lg k_1 + a \cdot \lg[RSH]_0 + b \cdot \lg[H^+]_0 \qquad 3.2.19$$

and can be used to obtain partial orders with respect to RSH or H^+. Therefore, at constant acidity, the slope of the regression line gives the reaction order with respect to RSH, whose excess was varied, and at constant excess of RSH and mineral acid varied, the order with respect to H^+. The combined figure III.2.7-8 illustrates those dependences.

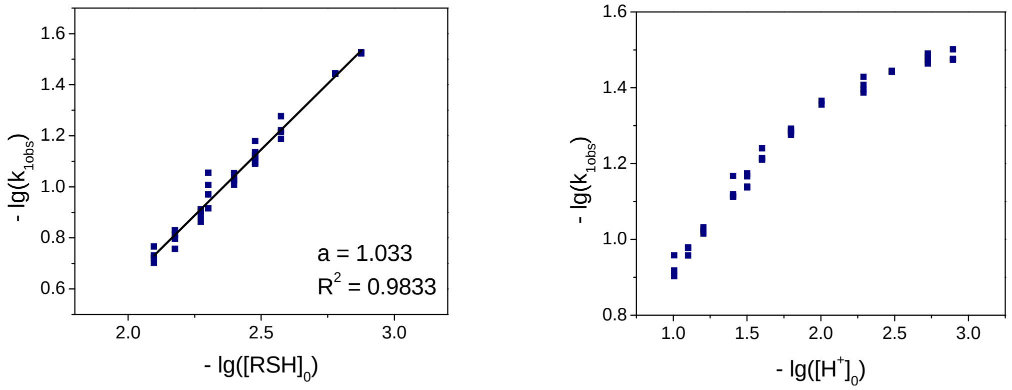

Figure III.2.7-8. Log – log plots to determine partial orders with respect to RSH and H^+.

The illustrated dependencies show a linear behavior on [RSH] with an integer 1.0 order, and a curve on $[H^+]$. At low acid concentration, the order with respect to hydrogen ion is near zero and increases as the concentration of the mineral acid is raised. This behavior appears systematic within all experimental conditions employed (various excesses of RSH and various temperatures). The reaction order in H^+ is fractional between zero and one, with an increasing trend as the acidity is increased. From a mechanistic point of view, this can be interpreted by the intervention of two concurrent reaction paths, one of zero order, and the other of first order in H^+, their relative importance being modulated by the range of acid concentration. The conclusion to be drawn from these facts and the micro-reversibility principle is that, the apparent first-order rate constant can be written as:

$$k_{1obs} = \left(k_1^0[RSH] + k_{-1}^0\right) + \left(k_1^H[H^+][RSH] + k_{-1}^H[H^+]\right) \qquad 3.2.20$$

Because these results were based on k_{1obs} obtained with relative large errors, they were verified by measurements with a technique for fast reactions. The kinetic curves recorded at

350 nm and extrapolated to zero time yield the initial rate expressed by the variation of absorbance with time:

$$r_{350nm} = -\frac{d[Cr(VI)]}{dt} = -\frac{1}{\varepsilon_R \cdot \ell}\frac{dA_{350}}{dt} = k_1[RSH]_0^a[H^+]_0^b[Cr(VI)]_0^d \qquad 3.2.21$$

By using various excesses of RSH and $HClO_4$, as well as several Cr(VI) concentrations (always as the limiting reactant), the following reaction orders were obtained from the double logarithmic plots of log r_0 as a function of log(concentration of varied species):

$HCrO_4^-$: 1.1 ± 0.1;   RSH: 1.02 ± 0.06 ; H^+: 0.68 ± 0.06

These results confirm the previous ones from the classical method of separation of the process into a sequence of two steps.

In order to evaluate the values of the rate constants the data under static conditions were analyzed. By plotting k_{1obs} as a function of excess thiol at constant acidity and as a function of acidity at constant thiol concentration the following figures were obtained:

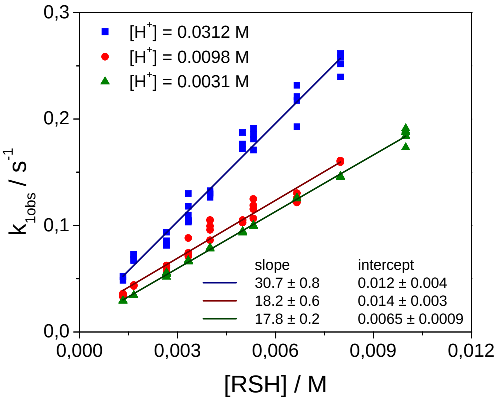

Figure III.2.10. Linear dependence on RSH with the slope $k_1^0 + k_1^H[H^+]$ (M^{-1} s^{-1})

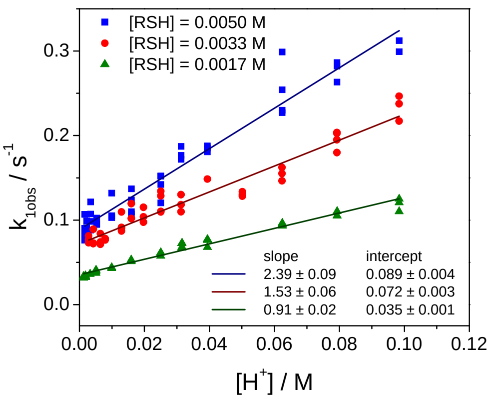

Figure III.2.11. Linear plots of k_{1obs} as a function of $[H^+]$ with the slope $k_{-1}^H + k_1^H[RSH]$ (M^{-1} s^{-1})

The intercepts in figure III.2.10 are slightly positive (statistically different from zero) but affected by large errors. Theoretically, they might represent the $k_{-1}^0 + k_{-1}^H[H^+]$ contribution to the apparent first-order rate constant. The slope is the $k_1^0 + k_1^H[H^+]$ ($M^{-1}s^{-1}$) term in $k_{1obs.}$ From these slopes rates of k_1^0 = (15±2) $M^{-1}s^{-1}$ and k_1^H= (5±1)·10^2 $M^{-2}s^{-1}$ were obtained for the formation of the intermediate in the path involving hydrogen ion. From the graph in figure III.2.11, with the intercepts differing from zero, it is obvious that there is a term having zero-order with respect to H^+ and another having first order in it. The same feature was observed under other different conditions. The linear regression parameters yield values of $k_1^0 = 16 \pm 3\ M^{-1}s^{-1}$ and $k_1^H = (4.4 \pm 0.4) \cdot 10^2\ M^{-2}s^{-1}$, in fairly good agreement with those obtained from the thiolactic acid concentration effect.

Kinetics of the electron transfer step (decay of the intermediate)

In order to determine reaction orders with respect to the reactive species, the apparent first-order rate constants k_{2obs} were used as dependent on the excess concentration of thiolactic acid or hydrogen ion concentration. Graphs of the type exemplified below were obtained under various conditions.

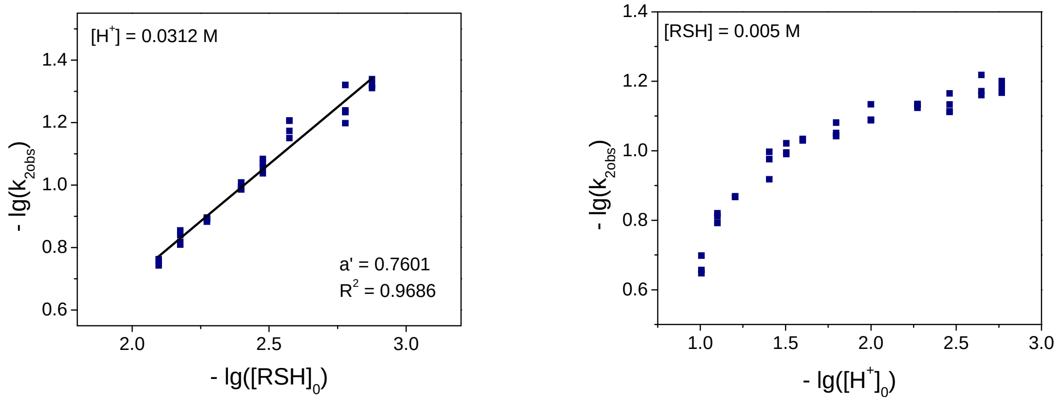

Figure III.2.12. Log-log plots to determine partial orders with respect to RSH and H^+

In the case of the organic substrate, the graphs were linear to a good approximation and a fractional order between zero and one was obtained in all cases. This observation can be interpreted as the concurrence of two processes, one of zero and the other of first order in RSH. From a mechanistic point of view this could be considered as a monomolecular decomposition of the intermediate, to form Cr(V) and a thiyl free radical $RS^\bullet$, along with a bimolecular process involving the complex and a new thiol molecule yielding the disulfide and Cr(IV) in an bi-equivalent electron transfer. On the other hand, the fractional order can be viewed as an expression of the *one-plus* form[301], $k_{2obs} = \alpha[RSH]/(1+\beta[RSH])$, as suggested by the presence of the pre-equilibrium of intermediate formation. This hypothesis is going to be tested in the following.

In the case of the involvement of hydrogen ions, once again there is a fractional order of less than 1, increasing with rising acidity, as in the case of formation of the intermediate $RSCrO_3^-$. These facts can be interpreted with two concurrent paths or by a *one-plus* dependence.

$$k_{2obs} = (k_2^0 + k_2^H[H^+])\frac{\alpha[RSH]}{1+\beta[RSH]} \qquad 3.2.22; \qquad k_{2obs} = \frac{\alpha[H^+][RSH]}{1+\beta[RSH]+\gamma[H^+]} \qquad 3.2.22'$$

The second form stipulates a decreasing effect of H^+ which was not found experimentally. The first form implies two parallel processes, meaning that a plot of k_{2obs} as a function of the acidity should yield a line with some positive intercept. It is so, as figure III.2.13 clearly demonstrates.

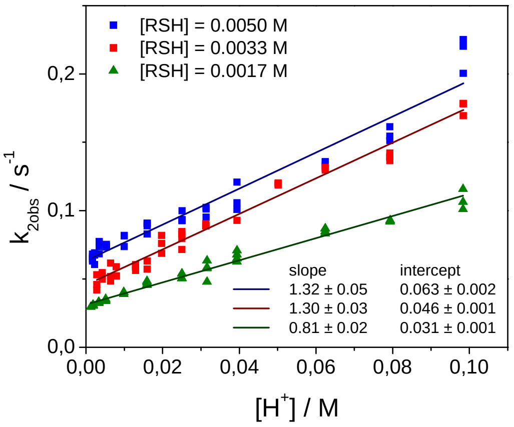

Figure III.2.13 Linear dependence of k_{2obs} on $[H^+]$

The accepted form of eq.3.2.22 stipulates that the slope and intercepts are:

$$\text{Slope=}k_2^H[H^+]\frac{\alpha[RSH]}{1+\beta[RSH]} \qquad 3.2.23; \qquad \text{Intercept=}k_2^0\frac{\alpha[RSH]}{1+\beta[RSH]} \qquad 3.2.23'$$

On the other hand, for the dependence of k_{2obs} on the organic substrate, equation 3.2.22 predicts a curved shape with the gradient diminishing as thiol concentration is increased. Such behavior was obtained, as it is seen in figure III.2.14. Also, lines of declining slopes were obtained when plotting the intercepts and the slopes in figure III.2.13 against the concentration of thiolactic acid, thus strengthening the belief in the truthfulness of this rate equation.

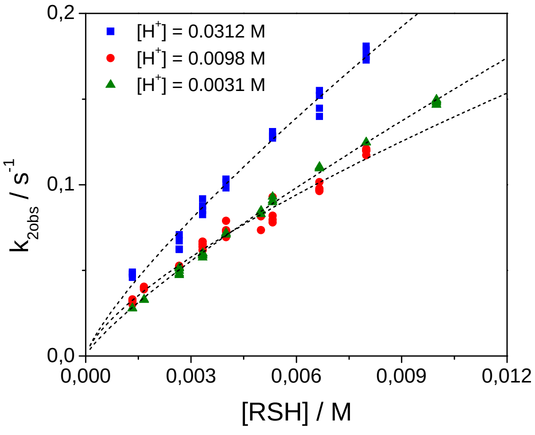

Figure III.2.14.
Dependence of k_{2obs} on thiolactic acid concentration

The increase of ionic strength showed no effect on the reaction of thioester complex formation while it diminishes the rate of its consumption. This is in agreement with the involvement of a neutral molecule in building of the intermediate, and some interaction of particles with opposite charges in its decomposition by a redox process.

Determination of activation energies

Because of the complexity of the system, only experimental activation energies could be determined from the dependence of either k_{1obs} or k_{2obs} with temperature. Seven temperatures, between 280 and 315 K were used at five perchloric acid concentrations. Nice Arrhenius plots were obtained with R^2 between 0.990 and 0.997. The results are given in table III.2.6.

Table III.2.6. Experimental activation energies (each figure has an error less than 2%)

$10^2\cdot[H^+]$ (M)	E_a (kJ/mol)	
	Intermediate formation	**Electron transfer step**
5.0	33.5	34.1
3.2	35.6	36.4
2.0	34.6	35.3
1.0	34.9	35.2
0.63	33.5	33.9
0.31	33.5	33.6
Mean:	34 ± 2	35 ± 3

Involvement of other intermediates

Because of the complexity of the system, some non-kinetic information was necessary. The literature brings proof of the implication of thiyl radicals in the majority of thiol oxidation reactions. Therefore we used the system to initiate the polymerization of methyl methacrylate. An increase in temperature of 1- 1.2 ºC was measured in a small calorimeter containing the reaction mixture and methyl methacrylate. At the end of the process, some polymer was isolated.

ESR spectra were also recorded in order to identify paramagnetic species, such as Cr(V) and thiyl radicals. The obtained results were compared to g values given in the literature. Working in a flow system, with $[Cr(VI)]_0 = 2.5\cdot10^{-3}$ M and $[RSH]_0 = 1.5\cdot10^{-2}$ M, the spectra presented in figure III.2.18 were obtained.

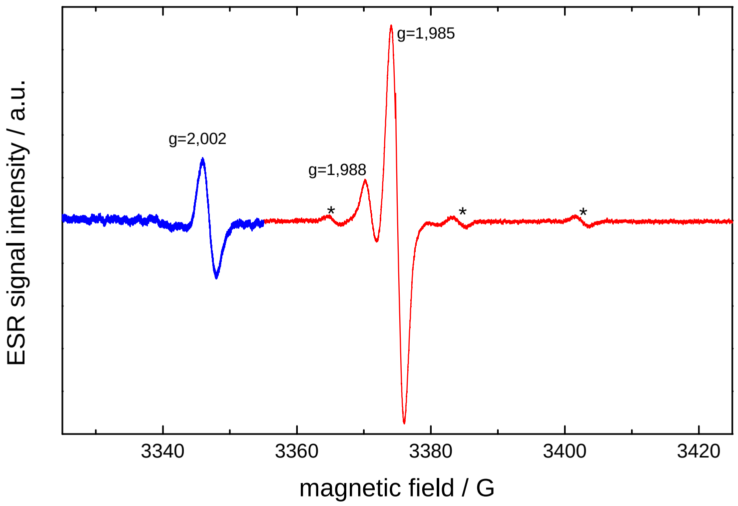

Figure III.2.18. Paramagnetic intermediates Cr(V) (red) and organic radical (blue). Signals marked with * are ^{53}Cr satellites of the principal signal at g = 1.985, with the last of the four expected lines overlapping with the signal of the organic radical at g = 2.002.

The species were assigned based on their g values: g = 1.985 and g = 1.988 were specific to oxo-complexes of Cr(V), and values g = 2.002 to an organic radical. It should be noted that the two parts of the spectrum shown in figure III.2.18 were recorded using different amplification settings of the ESR spectrometer.

In a stopped flow variant, at g = 1.985 and g = 2.002 kinetic curves were recorded taking the normalized intensity of the signals, as presented in figure III.2.19. Further discussion of the ESR results is given in the thesis.

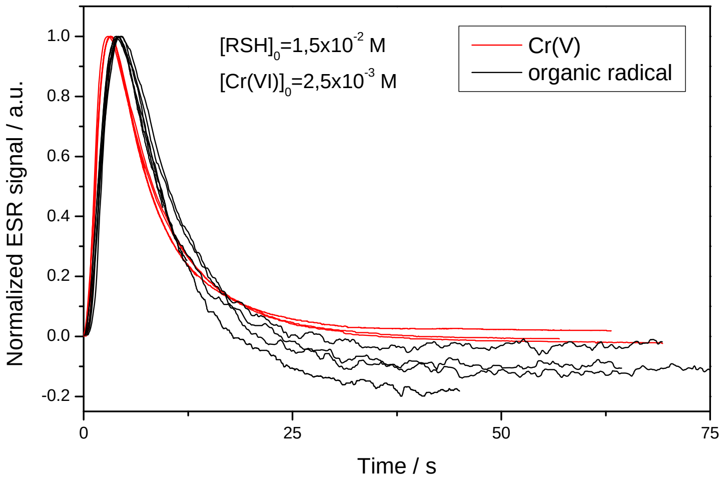

Figure III.2.19. Time evolution of the relative intensity of the signal for Cr(V) and the mixed one involving the organic free radical.

A surprising observation is that Cr(V) is not an extremely active species, its lifetime is rather long, in contrast to the majority of literature beliefs.

Discussions. Mechanism of the process

Based on the kinetic and extra-kinetic results presented, the following network of reactions is most probable:

$$RSH + HOCrO_3^- \rightleftharpoons RSCrO_3^- + H_2O \qquad k_{1,}^{0}\,k_{-1}^{0}, \quad K_f \tag{3.2.25}$$

$$RSH + HOCrO_3^- + H^+ \rightleftharpoons RSCrO_3^- + H_3O^+ \qquad k_{1,}^{H}k_{-1}^{H}, \quad K_f \tag{3.2.26}$$

$$RSCrO_3^- + RSH \longrightarrow Cr(IV) + RSSR \qquad k_{21} \tag{3.2.29}$$

$$RSCrO_3^- + RSH + H^+ \longrightarrow Cr(IV) + RSSR \qquad k_{22} \tag{3.2.30}$$

No precise affirmation can be made on the successive steps or rate-determining ones. To get the correct stoichiometry, Cr(IV) species should react further to form final products and generate Cr(V). The processes are characterized by higher rate constants and take place as fast as the corresponding intermediate species are formed, with the exception of the last one.

$$Cr(IV) + RSH \longrightarrow Cr(III) + RS^{\bullet} \tag{3.2.31}$$

$$Cr(IV) + Cr(VI) \rightleftharpoons 2\,Cr(V) \tag{3.2.32}$$

$$Cr(V) + 2\,RSH \longrightarrow RSSR + Cr\,(III) \tag{3.2.33}$$

An alternative, kinetically indistinct, with the rate determining steps as one-equivalent electron transfer and the formation of Cr(V) and a disulfide ion radical, is:

$$RSCrO_3^- + RSH \longrightarrow Cr(V) + RSSR^{-\bullet} \qquad k_{21}' \tag{3.2.34}$$

$$RSCrO_3^- + RSH + H^+ \longrightarrow Cr(V) + RSSR^{-\bullet} \qquad k_{22}' \tag{3.2.35}$$

The disulfide radical anion is a species with an electron in the anti-bonding S-S link, evidenced by β rays bombardment of thiol solutions[184] and is much more stable as compared to the thiyl radical, as determined in this work using MO calculations. The formation enthalpies are -254.3 kcal/mol for $RSSR^{-\bullet}$ and -64.19 kcal/mol for $RS^{\bullet}$.

The rate law deduced from each of the two variants of the mechanism is:

$$-\frac{d[HCrO_4^-]}{dt} = \frac{k_{21}K_f[RSH]^2}{1+K_f[RSH]}[HCrO_4^-] + \frac{k_{22}K_f[RSH]^2[H^+]}{1+K_f[RSH]}[HCrO_4^-] \tag{3.2.40}$$

in perfect agreement with the experimental one. Recall, that a first order with respect to thioester has been found, which contains one substrate molecule. Therefore the actual order with thiolactic acid is a fractional one, between 1 and 2. Taking into account the extra-kinetic proofs of the presence of free radicals, the stoichiometry and the Cr(V) implication, there should be sufficient arguments in favour of this mechanism.

III.3. THE OXIDATION OF THIOLACTIC ACID BY VANADIUM (V) IN ACIDIC MEDIUM[303]

The difficulties arising in oxidation with V(V) owe to the existence of numerous hydrolytic and acid-base equilibria involving this valence state, depending strongly on the solution pH and on the V(V) concentration. Monomer species like $VO_4^{3-}, HVO_4^{2-}, H_2VO_4^-, H_3VO_4$, and VO_2^+ as well as iso-polyvanadates such as $V_2O_7^{2-}, V_3O_9^{3-}, V_4O_{12}^{4-}, V_{10}O_{28}^{6-}, HV_{10}O_{28}^{5-}, H_2V_{10}O_{28}^{4-}$ are involved[92-98]. The decomposition and dissociation of decavanadate have been studied by spectrophotometrical means in basic[99.100], neutral and weakly basic[101] or acidic solutions[102.103], even from the kinetic point of view.

The purpose of this approach was to study the oxidation of thiolactic acid under conditions where the main species is decavanadate and vanadyl ion, respectively, and search for some reaction intermediates. Classic spectrophotometry was employed when the oxidant was $HV_{10}O_{28}^{5-}$ as it shows an intense yellow color[185]. Alternatively, stopped-flow measurements were performed, when comparable concentrations of VO_2^+ and thiolactic acid were used, but under the excess of H^+ ion.

Preliminary investigations

The stoichiometry of the reaction has been considered 2 $CH_3CH(SH)COOH$: 1 V(V), as Pickering and McAuley[216] determined for the oxidation of mercaptosuccinic acid. The products were disulphide and V(III) and this was confirmed by a spectrophotometrical titration.

To establish a wavelength at which the process can be monitored, spectra of $HV_{10}O_{28}^{5-}$ and VO_2^+ at a concentration of $2.22 \cdot 10^{-4}$ M expressed as monomer and thiolactic acid of $1.11 \cdot 10^{-2}$ M were compared. An important difference has been noticed at 340 nm. The monomeric species VO_2^+ reacts very rapidly, and require a method for fast reactions. On the other hand, the oxidation by decavanadate proceeds slowly an can be monitored by classical spectrophotometry.[298c,d]

The oxidation by decavanadate

Under the condition of a large excess of thiolactic acid (RSH) the evolution of the absorbance presents an exponential shape, as shown in figure III.3.2. It should be mentioned that, at the acidity employed in the measurements, acid hydrolysis of decavanadate takes place along with the oxidation process. This is also shown in figure III.3.2. As seen, the hydrolysis proceeds slower as compared to the oxidation. The acid hydrolysis obeys a first-order dependence on the concentration of the coloured species (decavanadate).

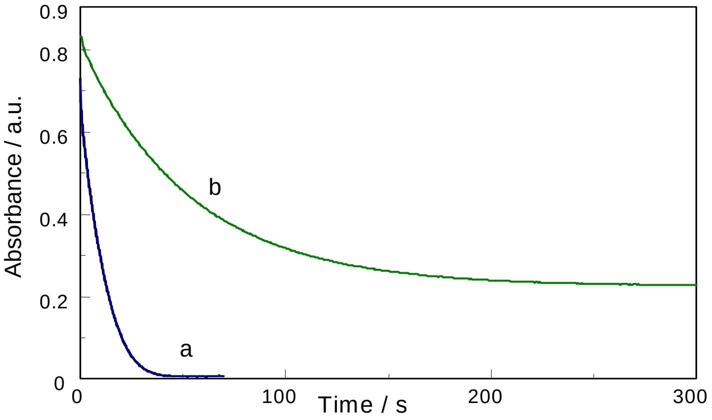

Figure III.3.2. Time-dependence of the absorbance for the acid hydrolysis (a) and combined redox + hydrolysis (b). Conditions: $[HV_{10}O_{28}^{5-}] = 2.22\cdot10^{-5}$ M, $[RSH] = 2.22\cdot10^{-2}$ M, $HClO_4 = 7.98\cdot10^{-2}$ M and $\mu = 0.5$ M at T = 293 K.

The corresponding semi-logarithmic plots were linear to more than 90 % of reaction.

$$\ln(A - A_\infty) = \ln(A_0 - A_\infty) - k_{h\,obs}t \qquad 3.3.1$$

Here, A, A_0 and A_∞ stand for absorbance at the time t, at the beginning and at the end of the process, respectively, and $k_{h\,obs}$ for the observed first-order rate constant of hydrolysis. This is in agreement with the data obtained by Clare and co-workers[195]. The same type of linear equation has been used for the overall hydrolysis and reduction by RSH process. It should be mentioned that the linear parts of such plots were only so for, at most, 1 unit of natural logarithm (about 25 % of the reaction). Within this range of V(V) conversion the correlation coefficients were in the range of 0.999 - 0.9999. The reason for such a behavior is seen in a higher reactivity towards reduction of the smaller poly-oxovanadates or monomeric forms. Both hydrolysis and redox processes release fragments of higher reactivity, resulting an increase of the reaction rate. This work shows that the VO_2^+ ion reacts quite rapidly. Its low concentration leads to the conclusion that it does not contribute significantly to the solution absorbance. By using the early part of the reaction it can be expected that the decavanadate species $HV_{10}O_{28}^{5-}$ is the one involved. The fact that the V(V) consumption by both hydrolysis and reduction by thiolactic acid proceeds faster that the hydrolysis itself indicates that also polymeric vanadates accept electrons, and thus not only the monomeric V(V) species, generated by the hydrolysis. Because the oxidation and hydrolysis take place simultaneously and both obey first-order kinetics, one can distinguish them by making the differences between the apparent first-order rate constants of the overall process and the hydrolysis.

$$k_{r\ obs} = k_{obs} - k_{h\ obs} \tag{3.3.5}$$

k_{obs} represents the first-order rate constant for redox process only. A combined table of III.3.1 and III.3.2 of the thesis contains the obtained values of the first-order rate constants under several experimental conditions.

Table III.3.1 and III.3.2 First order rate constants for overall process, hydrolysis and redox at various excesses of thiolactic acid and various perchloric acid concentration at ionic strength μ = 0.5 M, T = 293 K, $[HV_{10}O_{28}^{5-}] = 2.22 \cdot 10^{-5}$ M^{-1} ($2.22 \cdot 10^{-4}$ M^{-1} in $V(V)_{total}$). The values in the table are means of 3 to 4 kinetic runs.

$10^2[HClO_4]$ (M)	10^2[RSH] (M)	10^3 k_{obs} (s^{-1})	10^3 $k_{h\ obs}$ (s^{-1})	10^3 $k_{r\ obs}$ (s^{-1})
1.00	-	-	0.475	-
1.59	-	-	0.854	-
2.51	-	-	1.42	-
3.16	-	-	1.80	-
5.01	-	-	3.06	-
7.94	-	-	5.04	-
10.00	-	-	6.63	-
1.59	2.22	12.23		11.38
2.51	2.22	8.55		7.13
3.16	2.22	7.96		6.16
5.01	2.22	6.50		3.44
7.94	2.22	7.70		2.66
10.00	2.22	9.17		2.54
3.16	0.556	2.80		0.997
3.16	1.11	4.43		2.63
3.16	3.33	12.23		10.42
3.16	4.44	14.83		13.02
3.16	5.56	18.28		16.47

As seen from the data presented, the acid hydrolysis exhibits a linear dependence on the acidity. So it has been determined previously by Clare and co-workers[195] at higher H^+ concentrations and in nitric acid. The results of this work, when using $HClO_4$ as the hydrogen ion source, extend the first-order range towards lower acidities.

Concerning the redox process, a first-order dependence on the thiolactic acid concentration has been noted as shown in figure III.3.5, while the effect of the acidity on the rate is more complex, as depicted in figure III.3.7.

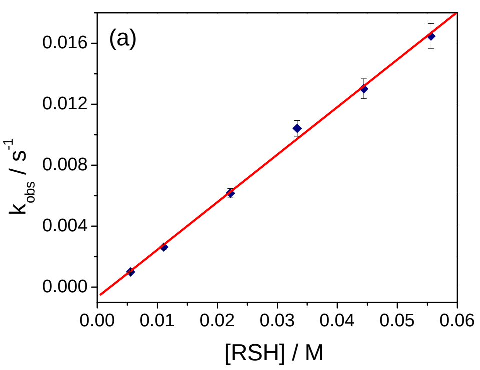

Figure III.3.5. The effect of thiolactic acid on the reaction rate. T=293, $[H^+]$= 0.316 $M^{-1}$and μ=0.5 M.

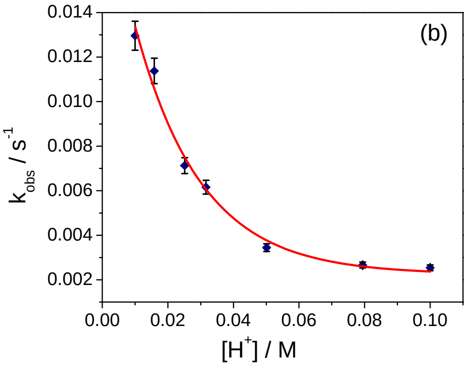

Figure III.3.7. Non-linear dependence of k_{obs} on H^+ ion concentration

The equation of the line at constant acidity is:

$$k_{obs} = -(0.0007 \pm 0.0003) + (0.312 \pm 0.009)[RSH] \qquad 3.3.6$$

confirming the first-order dependence on RSH. Figure III.3.7 indicates a negative (–1) order with respect to hydrogen ion concentration. If some intermediate complex V-thiolactic acid is involved, through a V-S bond, as proved by McAuley[216], then the thiol function is involved and it should be acid dissociated, which is in accordance with a negative order. A plot of k_{obs} as a function of $[H^+]^{-1}$gave a straight line.

Further experiments are needed in order to suggest a well-argued reaction mechanism. It is clear that some consecutive one-equivalent electron transfer steps are involved. The mixture changes its color to a pale-blue one, characteristic to V(IV) compounds, identified by ESR studies.

An attempt to determine activation parameters of the reactions has also been made. Measurements at three different temperatures (293, 303 and 313 K) have been undertaken, studying both the hydrolysis and the redox process, where the experimental activation energies of $E_{a\ h}$ = 61 ± 2 kJ.mol^{-1} and $E_{a\ redox}$ = 41 ± 3 kJ.mol^{-1} respectively, for the two reactions have been computed. Even if few, these measurements are trustworthy, as the value obtained for E_h is very similar to the one given by Clare at al[195] in nitric acid (75 kJ·mol^{-1}).

The oxidation by VO_2^+

Oscillograph traces, showing the disappearance of VO_2^+, were recorded at various concentrations of VO_2^+, RSH and H^+, the latter chosen in a concentration range ensuring that vanadium VO_2^+ was the predominant species. The reaction is completed within 1- 1.5 sec.

Reaction orders were determined, combining the isolation and the initial rate methods. That is, varying the concentration of one reactant while keeping the concentration of the others constant together with the ionic strength (0.1 M) and then, upon calculation of the initial reaction rate, determining the reaction order with respect to the varied reactant concentration, from classic log – log plots. The slope of the lines were 1.11 for RSH, 1.51 for VO_2^+ and −1.14 for H^+, representing the order on the specified reacting species. This corresponds to a first-order in RSH in the range of concentration ($2.5 \cdot 10^{-3}$ - $2.25 \cdot 10^{-2}$ M) at constant concentration of VO_2^+ ($2.5 \cdot 10^{-3}$ M), and − 1 with respect to H^+, within the narrow range of concentrations used, limited by the construction of the stopped-flow apparatus, which does not allow for more acidic solutions, and by the incomplete hydrolysis of the polymeric structure of the oxovanadium compound at lower acidities. Nevertheless, a clear trend towards decreasing rates with increasing pH was seen, allowing the estimation of the reaction order of H^+ as being -1. For VO_2^+ concentrations ranging from $5 \cdot 10^{-4}$ M to $3.5 \cdot 10^{-3}$ M at constant concentration of thiolactic acid ($1.13 \cdot 10^{-2}$ M), the method leads to an order of 1.5.

The influence of the ionic strength of the solution upon the reaction was also investigated, using fixed concentrations of the reactants, while applying ionic strengths of 0.1 to 1 M. It was found that the redox process suffers no influence of the ionic strength, as the plot shows no trend.

ESR investigations on the VO_2^+–thiolactic acid system.

The first ESR measurements were performed in continuous flow, attempting to identify paramagnetic species in the reaction of VO_2^+ ($2.5 \cdot 10^{-3}$ M) with thiolactic acid $7.5 \cdot 10^{-3}$ M, H^+ 0.032 M and ionic strength 0.1 M. They showed the presence of free V(IV), in moderate concentrations, at some stage of the reaction. This complies with some results reported in literature[214,215]. Figure III.3.12 shows the intensity of the ESR signal of the V(IV) compound at several times after mixing, showing that it decays in time.

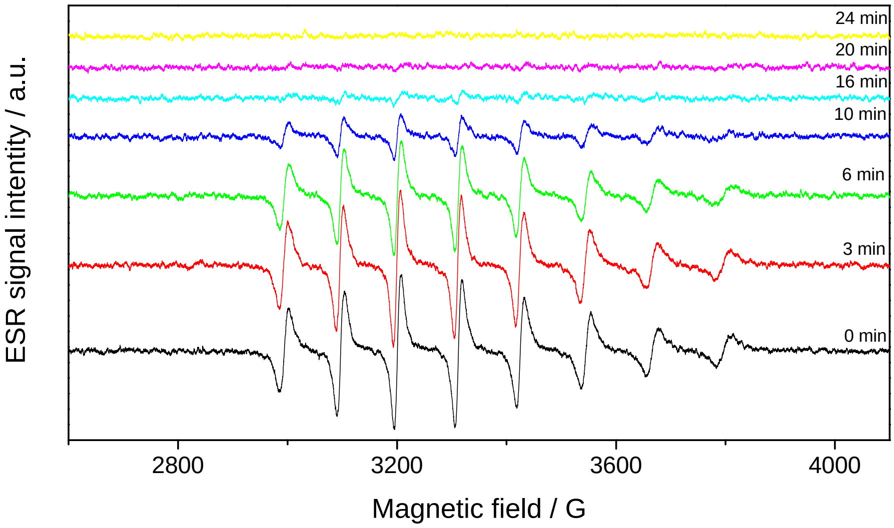

Figure III.3.12. ESR spectrum of V(IV) and its evolution in time.

The idea of comparing the results with those obtained for the oxidation of thiolactic acid by Cr(VI), prompted the search for organic radicals in the studied reaction. However, no such species were observed, due either to experimental limitations, or to the reaction itself, where the radical is formed in very low “steady-state” concentrations.

With identical experimental setup - only differing by the application of stopped-flow, kinetic curves were obtained. Good and reproducible kinetic curves were produced, but as this part of the study is still in its early stages results are sparse.

Conclusions

Although more data is needed to establish a reaction scheme, there are several obvious facts, such as: the rate expression, the occurrence of electron transfer involving polyoxovanadate, prior to the separation of a monomeric reactive form, the involvement of V(IV) which reacts not so rapidly as considered previously, and the lack of effect of ionic strengths. All these argue the presence of several parallel and consecutive steps: the formation of a 1 : 1 complex containing a S-V bond along with a 1 : 2 complex RSH : V(V) where the substrate is a bridge. Also, the formation of V(IV) in a one-equivalent electron transfer, which requires the formation of a free thiyl radical. On the basis of these results a probable sequence of reactions can be advanced, when the oxidizing agent is VO_2^+.

$$VO_2^+ + RSH \rightleftharpoons VO_2 - SR + H^+ \qquad K_1 \qquad 3.3.7$$

$$VO_2 - SR \longrightarrow V(IV) + RS^{\bullet} \qquad k_1 \qquad 3.3.8$$

$VO_2^+ + RSH \rightleftharpoons VO_2 - SR'COO - VO_2 + 2\,H^+ \quad K_2 \quad 3.3.9$

$VO_2 - SR'COO - VO_2 \longrightarrow V(IV) + RS^{\bullet} \quad k_2 \quad 3.3.10$

$V(IV) + RSH \longrightarrow V(III) + RS^{\bullet} + H^+ \quad k_3 \quad 3.3.11$

$2\,RS^{\bullet} \longrightarrow RSSR \quad 3.3.12$

Further ESR studies can bring information on the role of V(IV) in the reaction.

The mechanism of reaction with $HV_{10}O_{28}^{5-}$ should be, in a way, similar: the formation of an adduct that reacts and forms a V(IV) and a free thiyl radical and a cluster with one unit of V(V) less. Here, the large volume does not permit the formation of a 1:2 complex.

III.4. OXIDATION OF THIOLACTIC ACID BY HEXACYANOFERRATE(III) IN PERCHLORIC ACID MEDIUM[304]

Hexacyanoferrate (III) is well-known as a selective one-electron outer-sphere oxidant. The key step in the oxidation is an outer-sphere electron transfer, generally acknowledged to proceed by the formation of a substrate-oxidant ion-pair. Some electronic spectra obtained with mixtures of Fe(III) and Fe(II) of different ratios, compared to spectra obtained at various intervals of time in the presence of thiolactic acid argues the involvement of such a species.

Preliminary observations

Reaction stoichiometry. The oxidation of thiolactic acid (abbreviated as RSH) by hexacyanoferrate (III) proves to have a $1[Fe(CN)_6]^{3-}$: 1 RSH stoichiometric ratio, as found by spectrophotometrical titration (figure III.4.1).

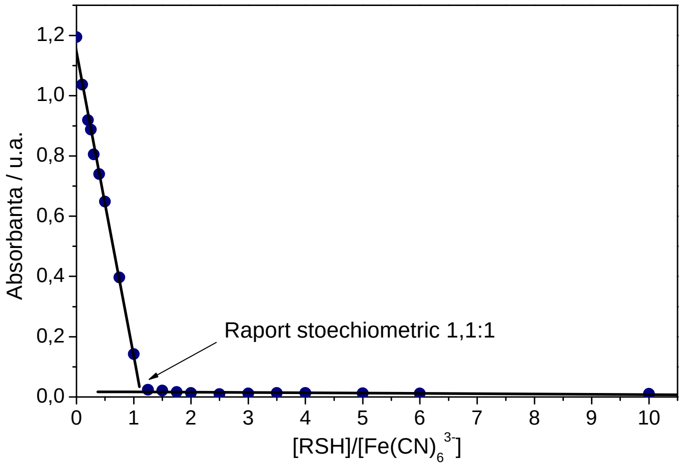

Figure III.4.1. Remaining absorbance of $[Fe(CN)_6]^{3-}$ after the reaction with thiolactic acid has been accomplished.

This indicates that the oxidation of thiol-acid to the corresponding disulphide takes the following form:

$$2HFe(CN)_6^{2-} + 2CH_3CH(SH)COOH \rightarrow 2HFe(CN)_6^{3-} + (HOOCCH(CH_3)S)_2 + 2H^+ \qquad 3.4.1$$

Kinetics

The kinetic approach employed pseudo-first-order conditions (excess concentrations of the substrate and the hydrogen ion as well as a constant ionic strength $\mu = 0.5$ M). Indeed, a linear plot obeying a semi-logarithmic equation has been found, for all but the initial part. The linearity was quite good (R^2 between 0.9980 and 0.9999), implying a first-order behavior of the absorbing species (hexacyanoferrate(III) and its outer-sphere ion-pair intermediate).

Our interest focuses on the influences exhibited by the thiolactic acid and hydrogen ion on the pseudo-first-order constant, describing the electron-transfer process. Such rate coefficients have been obtained from the linear part of semi-logarithmic plots of the type $\ln(A-A_\infty) = f(t)$, and are collected in part in table III.4.1 (the number of replicate runs are specified in parenthesis). Series of measurements have been performed at 3 constant acidities while varying the thiolactic acid concentration and then for 3 excess concentrations of RSH while the acidity was varied. In both cases the outcome was a complex behavior.

Table III.4.1. First order rate constants at 293±0.1 K, μ=0.5 M and $[[Fe(CN)_6]^{3-}] = 2.22\ 10^{-4}$M, as a function of 2-mercapto-propionic acid concentration for 3 different excess concentrations of $HClO_4$ and as a function of $[H^+]$ for 3 different excess concentrations of the thiol - acid.

10^2 [*RSH*] (M)	**[H^+] (M)**			**10^2 [H^+] (M)**	**[*RSH*] (M)**		
	0.32	**0.10**	**0.032**		**0.011**	**0.017**	**0.022**
	$10^3\ k_{obs}$ (s^{-1})	**$10^3\ k_{obs}$ (s^{-1})**	**$10^3\ k_{obs}$ (s^{-1})**		**$10^3\ k_{obs}$ (s^{-1})**	**$10^3\ k_{obs}$ (s^{-1})**	**$10^3\ k_{obs}$ (s^{-1})**
0.44		0.36 (6)	2.96 (3)	15.85	0.94 (6)	2.14 (3)	2.87 (3)
1.11		2.29 (11)	18.80 (11)	12.59	1.45 (5)	2.93 (3)	4.48 (3)
1.67		4.42 (9)	36.02 (6)	10.00	2.29 (11)	4.42 (9)	7.41 (14)
2.22		7.41 (14)	61.46 (7)	7.94	3.66 (7)	6.91 (3)	10.29 (6)
2.78	1.69 (4)	11.68 (7)	96.95 (6)	6.31	5.10 (10)	10.27 (3)	15.16 (6)
3.33	2.49 (5)	16.81 (13)	124.96 (5)	5.01	8.08 (8)	14.92 (4)	22.00 (4)
3.89	3.40 (4)	22.59 (8)	156.36 (7)	3.98	13.81 (8)	22.14 (3)	37.36 (5)
4.44	4.38 (5)	28.44 (9)	194.23 (6)	3.16	18.80 (11)	36.02 (6)	61.46 (7)
5.00	5.38 (5)	35.90 (3)	206.86 (5)	2.51	30.23 (6)	51.89 (4)	84.31 (5)
5.56	6.54 (7)	48.44 (5)	286.91 (8)	2.00	42.42 (7)	78.24 (3)	120.66 (3)
				1.58	63.36 (9)	114.04 (3)	170.84 (7)

When the concentration of thiolactic acid was varied, the log – log plots were linear with slopes of quite similar values, but being slightly smaller than 2 (1.893, 1.95 and 1.74 for concentrations of mineral acid of 0.5 M, 1.0 M and 1.5 M, respectively). The second-order representations were not satisfactory, as they exhibited negative intercept or obvious curvature. Thus a fractional order between first- and second-order with respect to thiolactic acid has been considered. This behavior can be described fairly well by a *one-plus* form of the rate expression. No occurrence of curvature was observed in the *one-plus* type plot; along with the slightly improved correlation coefficients it favors this approach. The corresponding equations are shown below:

$$k_{obsd} = \frac{k_a[RSH]^2}{1 + k_b[RSH]} \qquad 3.4.4 \qquad\qquad \frac{[RSH]}{k_{obsd}} = \frac{1}{k_a}\frac{1}{[RSH]} + \frac{k_b}{k_a} \qquad 3.4.5$$

where k_a and k_b are combinations of rate constants of the elementary steps involved in the reaction mechanism. Figure III.4.5 shows the linear behavior, described by eq.3.4.5.

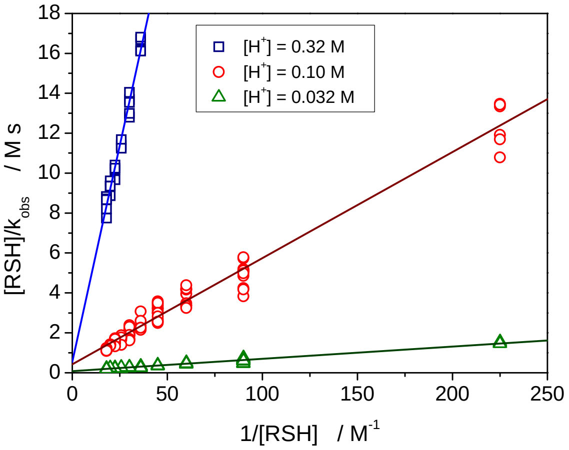

Figure III.4.5. Linear form of *one-plus* rate law at three constant acidities

When the hydrogen ion concentration was varied at constant concentration of thiolactic acid, the corresponding log–log plots showed an intermediate negative order, between -1 and -2 (-1.87, -1.74 and -1.82, when $[RSH]_0$ was 0.011 M, 0.017 M or 0.022 M respectively). This provides strong evidence for an interpretation in the light of *one-plus* type plots whose linear form is

$$\frac{1}{k_{obs}[H^+]} = \frac{1}{k_a^{'}}[H^+] + \frac{k_b^{'}}{k_a^{'}} \qquad 3.4.6$$

Figure III.4.7 shows good linear plots of the above given equation.

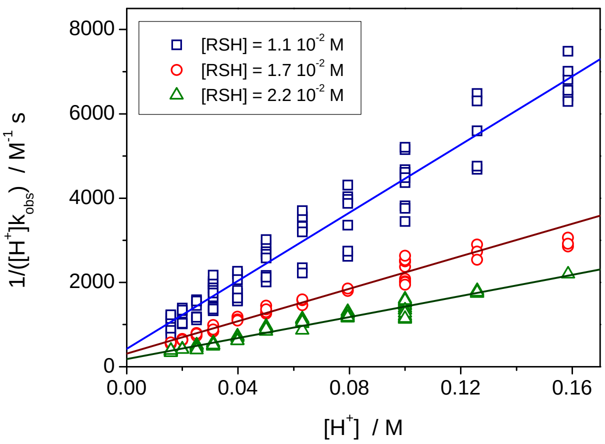

Figure III.4.7. The effect of the acidity on the first-order rate constant, eq.3.4.6.

The temperature effect has been checked in the range 283 – 313 K and $[H^+] = 0.1$ M, $[RSH] = 2.22\cdot10^{-2}$ M and constant ionic strengths of 0.5 M. A good Arrhenius plot has been obtained and an experimental activation energy of 10.6±0.5 $kJ.mol^{-1}$ has been computed from the slope of the line. This is a rather small value, indicating the presence of an exothermic pre-equilibrium.

Presence of free radicals. The involvement of free radicals in the overall process has been proved by the initiation of polymerization of methyl methacrylate by the redox system. An increase of temperature due to polymerization has been measured in a small calorimeter containing reacting mixture and monomer. Also, at the end, some polymer could be isolated.

Reaction mechanism.

The experimental results comprising reaction orders, the *one-plus* rate law, spectral evidence of the involvement of an outer-sphere intermediate and free radicals led to the following proposed sequence of steps:

$$\mathrm{RSH} \rightleftharpoons \mathrm{RS^- + H^+} \qquad K_1 \tag{3.4.8}$$

$$[\mathrm{Fe(CN)_6}]^{3-} + \mathrm{RSH} \rightleftharpoons \left([\mathrm{Fe(CN)_6}]\cdot\mathrm{SR}\right)^{4-} + \mathrm{H^+} \qquad K_2 \tag{3.4.9}$$

$$\left([\mathrm{Fe(CN)_6}]\cdot\mathrm{SR}\right)^{4-} + \mathrm{RS^-} \longrightarrow [\mathrm{Fe(CN)_6}]^{4-} + \mathrm{RS \therefore SR^-} \qquad k,\ r.d.s. \tag{3.4.10}$$

$$\mathrm{RS \therefore SR^-} + [\mathrm{Fe(CN)_6}]^{3-} \longrightarrow \mathrm{RS : SR} + [\mathrm{Fe(CN)_6}]^{4-} \tag{3.4.11}$$

The reactive species is the outer-sphere complex, which undergoes electron transfer assisted by a new de-protonated thiolactic molecule to form a short-lived disulphide radical anion, which is more stable than a thiyl radical. It reacts as quickly as it is generated with hexacyanoferrate (III) to give the final oxidation product, the disulphide.

The rate law deduced from this mechanism, when $[Fe(III)]_t$ is followed by the change of solution color at 420 nm, is of the form *one-plus* and explains the dependence on both [RSH] and $[H^+]$.

$$\frac{d[Fe(III)]_t}{dt} = \frac{kK_1K_2[RSH]^2/[H^+]}{[H^+]\{1+K_2[RSH]/[H^+]\}}[HFe(CN)_6^{2-}] \qquad 3.4.16$$

The linear form of the observed first-order rate coefficient as dependent on both RSH and H^+ is:

$$\frac{[RSH]}{k_{obs}[H^+]} = \frac{1}{kK_1K_2}\frac{[H^+]}{[RSH]} + \frac{1}{kK_1} \qquad 3.4.17$$

Such a line was obtained (Figure III.4.10) with all data at the same temperature, with a relatively good correlation coefficient (0.9707).

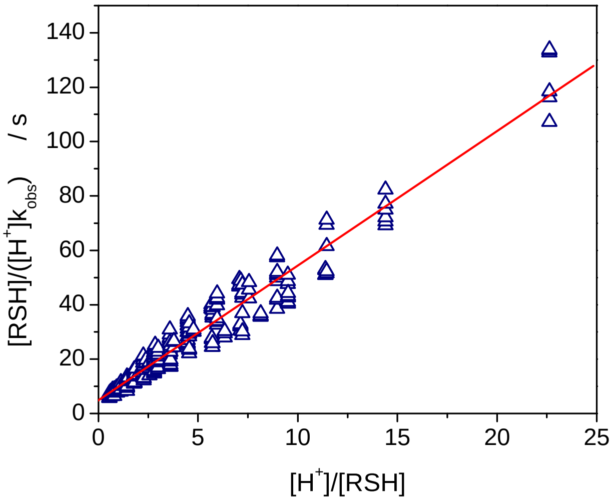

Figure III.4.10. Linear dependence described by eq.3.4.17, deduced from the suggested mechanism.

From the linear regression parameters (y = (4.9±0.4) + (4.95±0.079)x) it was possible to compute K_2 = 0.99±0.09 and kK_1= 0.2 ±0.02s^{-1}, thus proving that the advanced reaction network seems to be probable.

Conclusions

As presented by the studied reaction, the experimental kinetic data obey *one-plus* rate laws, with the integer exponents. A pre-equilibrium involving an outer-sphere complex between the oxidant and the organic substrate is present and the electron transfer is the rate-determining step. In acidic media, the involvement of hydrogen ion inhibits the oxidation of hexacyanoferrate(III). Phenomenological rate coefficients and some intermediate formation constants could be calculated. The data fit well with the rate law deduced from the reaction schemes, thus supporting the suggested mechanisms. Extra-kinetic proofs also account for the reaction network.

III.5. THE OXIDATION OF GLUTATHIONE BY CR(VI) IN AQUEOUS PERCHLORIC ACID SOLUTIONS[305]

The oxidation reaction of glutathione has been studied under similar conditions as those used for the reaction between thiolactic acid and chromate. Conventional spectrophotometry could be employed because the redox process proceeds more slowly as compared to the thiolactic acid oxidation.

Preliminary observations.

During the mixing of reactant solutions the color changes to a reddish-brown one, which pales slowly to colorless within several hours. It means a long-lived intermediate is rapidly formed. Figure III.5.1 presents comparative spectra of $HCrO_4^-$ and of the mixture during time of reaction, proving the formation of the intermediate.

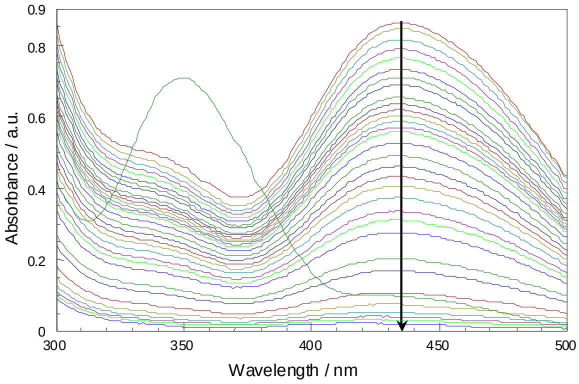

Figure III.5.1. Mixture spectra at various times after mixing as compared to $HCrO_4^-$ ($4.7\cdot10^{-4}$ M), T=293 K, $[Cr(VI)]_0 = 5\cdot10^{-4}$ M, $[GSH]_0 = 3.33\cdot10^{-3}$ M, $[H^+] = 3.67\cdot10^{-2}$ M and $\mu \approx 0.037$ M.

Here, the abreviation of glutatione is GSH, as it is usual in literature. The maximum position of the band is located at 435nm. The batochromic shift as compared to that of Cr(VI) proves the formation af a S−Cr bond in an 1 : 1 complex , in accordance with literature data[176,177,179,183] and the findings in the previous section. This formation is quite rapid and cannot be followed by classical spectrophotometry, and therefore this part of the reaction has been approached using a stopped-flow technique.

KINETICS

Formation of the intermediate complex. If the reaction is monitored at very short times (the conversion at most 2%[300]) the rate expressed by the modification of absorbance A_{435}, depends upon the initial reactant concentrations as:

$$r_{435nm} = \frac{dA_{435}}{dt} = \alpha[GSH]_0^a[H^+]_0^b[Cr(VI)]_0^c \tag{3.5.1}$$

where α contains rate constant and molar absorbance, and the exponents are reaction order with respect to the reactants. Now, experiments were carried out at constant concentration of two species and the remaining one was varied in turn. Whether the rate measured was represented as a function of varied species concentration, or double logarithmic plots were made, straight lines were obtained, as exemplified by the figures below. The dependence found is in agreement with first order in each of Cr(VI), GSH and the acidity

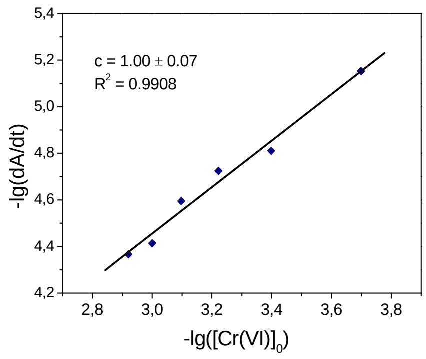

Figure III.5.3 Determination of the reaction order with respect to Cr(VI). ($[GSH]_0 = 0.004$ M; $[H^+]=0.0257$ $[Cr(VI)]_0=0.0002 \div 0.0012$ M)

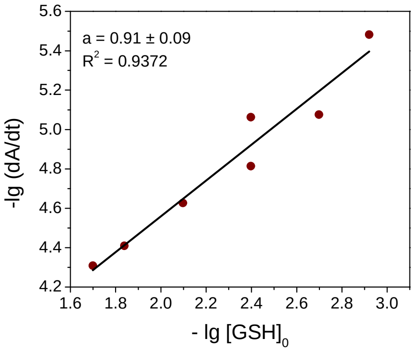

Figure III.5.4. Determination of the reaction order with respect to GSH ($[Cr(VI)]_0=0.0004$ M; $[H^+]=0.0257$ M; $[GSH]_0=0.0012 \div 0.02$ M)

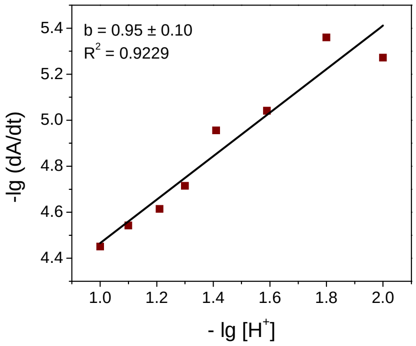

Figure III.5.5. Determination of the reaction order with respect to $[H^+]$.($[GSH]_0 = 0.004$ M; $[Cr(VI)]_0=0.0004$; $[H^+]=0.0257 \div 0.1$ M)

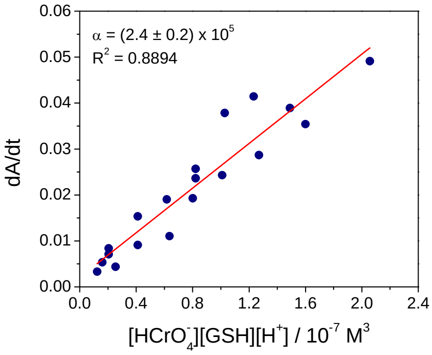

Figure III.5.6. Overall dependence of the rate ($[GSH]=0.004$ M; $[Cr(VI)]_0=0.0004$ M; $[H^+]=0.01 \div 0.1$ M)

By taking into account the path lengths of the observation cell in the stopped-flow device of 0.336 cm, the molar absorptivity of Cr(VI) species is determined from the slope of the line obtained by representing A_0 as a function of $[Cr(VI)]_0$. A value of $\varepsilon = 227 \pm 4\ M^{-1} \cdot cm^{-1}$ has been obtained, in good agreement with literature data for $HCrO_4^-$ species.

Decay of the intermediate complex. Studies on this redox process have been carried out by monitoring the evolution of absorbance at 435 nm. The curve exhibits a bi-phasic shape, with the first part progressing much more rapidly as compared to the disappearance of the condensed complex, as shown in figure III.5.7

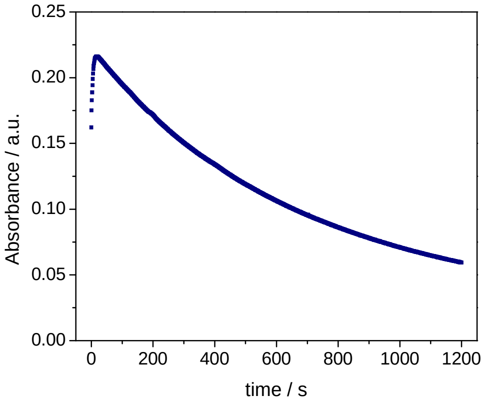

Figure III.5.7. An experimental bi-phasic evolution of absorbance at 435 nm. T = 293 K, $[Cr(VI)]=1.33 \cdot 10^{-4}$ M, $[GSH]=1.33 \cdot 10^{-2}$ M, $[H^+]=2.97 \cdot 10^{-2}$ M and $\mu=0.5$ M.

The second part of the reaction seemingly exhibits an exponential dependence. Indeed, the logarithmic form gave straight lines with the slope k_{2obs} proving the first-order dependence upon $GSCrO_3^-$. When the concentration of substrate was varied at constant acidity, or the hydrogen ion concentration was varied at constant glutathione concentration, complex dependencies were found. A fractional order between zero and one (nearer to unity) has been found from the double-logarithmic plot. The interpretation of this consists of either the occurrence of two reaction paths, one of zero order and the other of first order with respect of GSH, or a dependence of a *one-plus* type in the rate expression. This finding is similar to that of the thiolactic acid – chromate system. The same similarity occurs with the effect of hydrogen ion concentration. The double-logarithmic plot exhibits a fractional sub unitary and increasing order with the acidity. It means that as the concentration of hydrogen was raised, a reaction pathway involving H^+ became more important. Therefore two concurrent reaction paths, one without hydrogen ion, and another with it, are operating in the redox process.

An ***experimental activation energy*** of $E_a = 40 \pm 1\ kJ \cdot mol^{-1}$ has been obtained from the k_{2obs} values determined at 6 values of temperature in the range of 293 - 323 K.

The involvement of paramagnetic intermediates.

ESR measurements were made in a static regime at temperatures of 277 K and 293 K. The results showed that several Cr(V)-Glutathione complexes are formed during the overall process. The complex species and their lifetime depend upon the acidity. Figure III.5.11 presents these ESR signals.

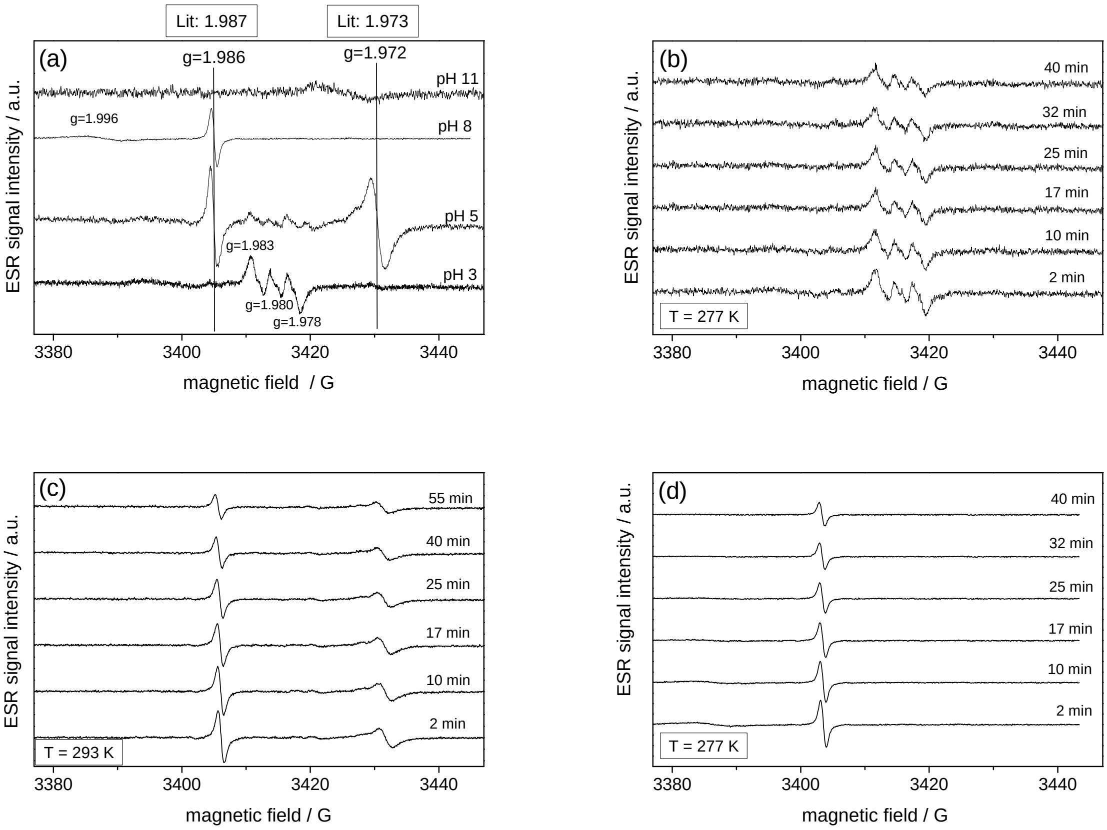

Figure III.5.11. Complexes Cr(V)-glutathione present in the reaction mixture at various acidities (a) and time evolution of the height of the ESR signal at pH 3 (b), 5 (c) and 8 (d).

The intermediates persist in solution at 293 K either by stabilization upon complexation with the excess substrate, or reaching a steady-state concentration.

Organic radical intermediates fail to evidentiate, possibly because of very low steady-state concentration due to their great reactivity.

Conclusions

Taking into account the similarities of this systerm with the one of thiolactic acid - Cr(VI) concerning the dependence of the aparent first order rate constant on the substrate and hydrogen ion concentration, as well as the involvement of Cr(V) species, there are enough arguments to consider similar rate equation and sequence of elementary steps in the overall process.

III.6. THE OXIDATION OF α-TOLUENETHIOL BY CHROMATE IN ACETIC ACID[306]

This case involves a substrate with thiol function linked to a primary carbon atom, which is bound to a phenyl radical. This bulky group, as well as the presence of the oxidizing agent in the form of condensed species acetochromate[110b)] $CH_3COOCrO_3^-$ bring about the involvement of electronic and steric effects on the rate, making the study of interest from this point of view.

Preliminary observations.

The stoichiometry of the oxidation is 3 Toluenethiol : 1 Cr(VI) as confirmed by a spectrophotometrical titration at 350 nm, using constant Cr(VI) concentration and increasing thiol concentration.

In mixing the thiol solution and acetochromic acid solution, the yellow-orange color of the Cr(VI) solution instantly turned to grey-green during the mixing time. Then, this color vanished steadily and rapidly towards a colorless solution.

The electronic spectrum of the mixture was recorded point by point at 10 s after mixing by means of a Zeiss Spekol spectrophotometer and compared to that of acetochromic acid as presented in figure III.6.1

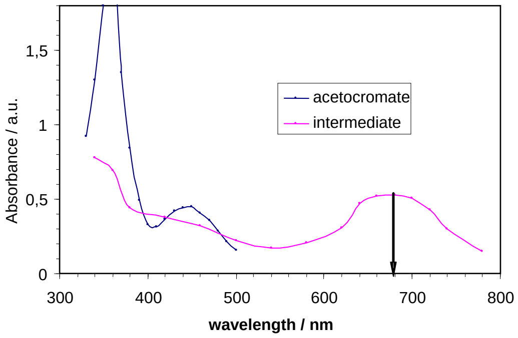

Figure III.6.1. The qualitative spectrum of the intermediate at 10 s after mixing . ($[Cr(VI)]_0 = 5\cdot10^{-4}$ M and $[C_6H_5CH_2SH]_0 = 1.79\cdot10^{-2}$ M), as compared to that of acetochromic acid ($5\cdot10^{-4}$ M).

The bonding of the central atom to a sulphur ligand, proving the formation of such position of charge-transfer band from oxygen as ligand to Cr(VI) shifted largely from 348 to 680 nm by an intermediate[176,177,179,183]

$$C_6H_5CH_2SH + HOCrO_2OAc \rightleftharpoons C_6H_5CH_2SCrO_2OAc + H_2O \qquad 3.6.2$$

To consider the formation and decay of this intermediate, some spectra of the mixture were recorded during the reaction every 4.5 seconds by means of a photodiode-array spectrophotometer as presented in figure III.6.2.

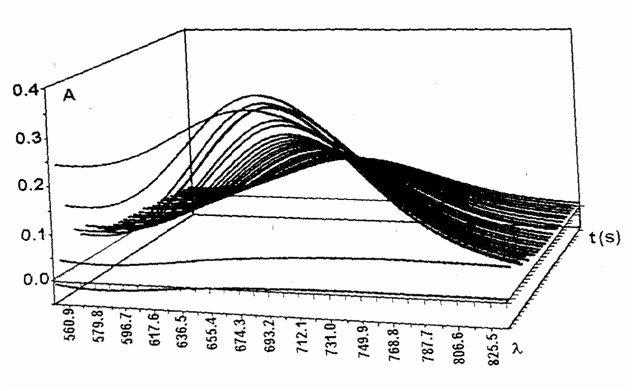

Figure III.6.2. Absorption spectra of the mixture containing initial concentration of $5 \cdot 10^{-4}$ M Cr(VI) and $2.49 \cdot 10^{-2}$ M $C_6H_5CH_2SH$ in acetic acid during time. The path length of the cuvette was 1 cm.

Even the first spectrum is different than that of acetochromic acid, confirming the maximum at 680 nm and the fast formation of the intermediate. The decay of this species is quite rapid, in the order of one to two minutes.

The kinetics of the process.

All measurements make use of pseudo-first-order conditions (quite large excess of α-toluenethiol). The process of diminishing absorbance either at 350 or 680 nm exhibits an exponential profile, with the exception of the first several points. This first part corresponds mainly to the formation of the intermediate.

Therefore, the linear form of the absorbance evolution gave straight lines according to equation 3.6.3.

$$\ln(A - A_\infty) = \ln(A_0 - A_\infty) - k_{2obs} \cdot t \qquad 3.6.3$$

The values A, A_0 and A_∞ stand for the actual reading, the initial and final reading of absorbance, respectively.

The slope of the line is equal to the rate constant k_{2obs} (s^{-1}) of the redox process. Good correlation coefficients were obtained with such linear regressions. Table III.6.1 collects several means of the apparent first-order rate constants, each obtained from 4 - 5 individual runs under identical conditions, at 680 nm.

Table III.6.1. Mean rate constants at the decay of the intermediate through electron transfer (at 680 nm).

$10^2 \cdot [C_6H_5CH_2SH]$ (M)	$10^2 \cdot k_{2obs}$ (s^{-1})	R^2
1.12	2.89 ± 0.03	0.9988
0.56	2.75 ± 0.05	0.9910
0.28	2.96 ± 0.40	0.9823
0.224	3.04 ± 0.40	0.9831

The results were the same as seen with several kinetic runs followed at 350 nm, where the decrease of absorbance is due to both the acetochromic acid and the intermediate thioester. Here, as in the previous systems approached in the thesis, the rapid formation of the condensed species in a pre-equilibrium is followed by its decay. Under a large excess of the reducing agent, the overall process can be shown to be the sequence of two first order processes $R \xrightarrow{k_{1obs}} I \xrightarrow{k_{2obs}} P$ in which $k_{1obs} = k_1 [C_6H_5CH_2SH] + k_{-1}$ and R, I and P stand for acetochromic acid, the thioacetochromate intermediate and the final product, respectively. This system has been treated classically, similar to the system thiolactic acid –chromate in section III.2.4. Therefore, the absorbance evolution is described by the equation $A - A_\infty = \gamma_1 e^{-k_{1obs}t} + \gamma_2 e^{-k_{2obs}t}$. Its linear form, at the values of time where the first exponential vanishes, becomes $\ln(A - A_\infty) = \ln \gamma_2 - k_{2obs} \cdot t$. The apparent first-order rate constant for the consumption of thioester was determined from the slope of the line (equation 3.6.3 rewritten in this fashion). For the initial part of the run, where the decomposition of intermediate has not yet an important contribution, another linear equation can be written, making use of the parameters of the line describing the decay process

$$\ln(A - A_\infty - \gamma_2 e^{-k_{2obs}}) = \ln \gamma_1 - k_{1obs} \cdot t \qquad 3.6.8$$

Figure III.6.5 shows the linear dependence described by the equations 3.6.3 and 3.6.8, and the results (as the slope of the lines) are collected in table III.6.2.

Table III.6.2. First-order rate constants for the two consecutive processes at 288 K and $[Cr(VI)] = 5.0 \cdot 10^{-4}$ mol/L.

$10^2 [C_6H_5CH_2SH]$ (M)	k_{1obs} (s^{-1})	R^2	$10^2 k_{2obs}$ (s^{-1})	R^2
1.39	0.17 ± 0.02	0.9773	2.95 ± 0.04	0.9992
1.12	0.16 ± 0.01	0.9880	3.16 ± 0.07	0.9984
0.84	0.154 ± 0.003	0.9986	2.94 ± 0.07	0.9988

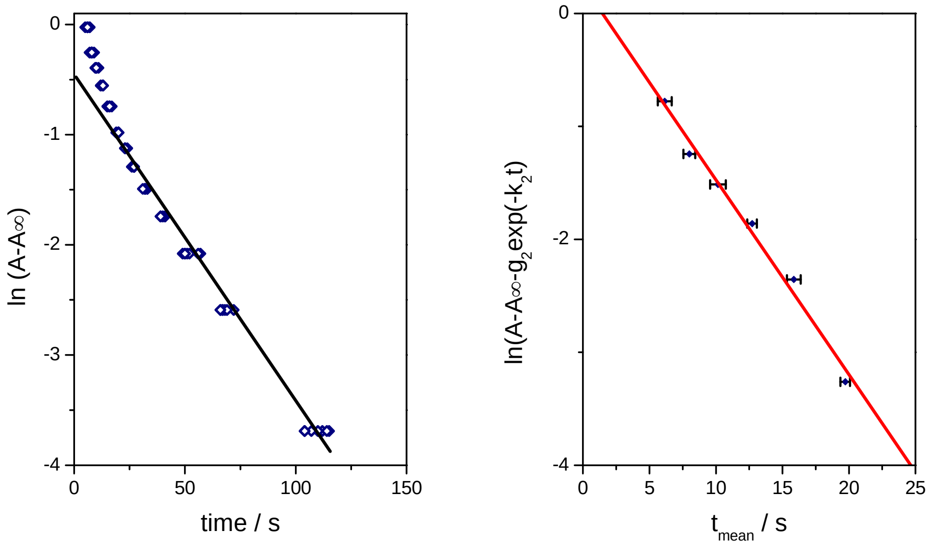

Figure III.6.5. Linear dependence as described by the equations 3.6.3 and 3.6.8. [Cr(VI)] = 5,0 x 10^{-4} M and [$C_6H_5CH_2SH$] = 1,12 x 10^{-2} M, at 360 nm and 288 K. (The points exemplify the distribution of values, linear regression was calculated with mean times in order to reach a particular absorbance value)

As seen in the tables III.6.1 and III.6.2, the rate coefficient k_{2obs} does not depend on the substrate concentration, the redox process of intermediate consumption exhibits zero–order with respect to α-toluenethiol. On the other hand, it is seen that the condition for applying the classic method $k_{1obs} \geq 5\, k_{2obs}$ is fulfilled. A similar behavior has been found in the case of thiophenol oxidation.[109]

A trend of increasing k_{1obs} with increasing thiol concentration has been expected. Although more data are necessary, a plot of k_{1obs} as a function of α-toluenethiol concentration exhibits a linear dependence with the intercept different of zero. From the parameters of the line $k_{1obs} = k_1\ [C_6H_5CH_2SH] + k_{-1}$, values of $k_1 \approx 2.7\pm1.3\ M^{-1}s^{-1}$ and $k_{-1} \approx 0.13\pm0.02\ s^{-1}$ have been estimated at 288K as well as an apparent equilibrium constant of 21 ± 13 M^{-1}.

The effect of temperature on k_{2obs} was investigated at four temperature values between 288 and 308 K, following the process at 680 nm. Excellent lines were obtained with R^2 between 0.9984 and 0.9986, and rate coefficients calculated. Using these values and the linear form of the Arrhenius and Eyring equations, the following activation parameters were obtained: E_a= 50.9±1.3 kJ.mol^{-1}, $\Delta H^{\neq}$ = 48.4± 1.3 kJ.mol^{-1} and $\Delta S^{\neq}$ = –106 ±5 J.$mol^{-1}K^{-1}$. The negative and relative large value of activation entropy is in agreement with the formation of a condensed compound.

The equilibrium constant of thioester formation

Two methods were employed for the calculation of the apparent equilibrium constants

$$K' = \frac{K}{[H_2O]} = \frac{[C_6H_5CH_2SCrO_2OAc]}{[HOCrO_2OAc][C_6H_5CH_2SH]} = \frac{x}{(a\text{-}x)(b\text{-}x)} \qquad 3.6.9$$

Recording the decay of thioester by means of absorbance at 680 nm, the kinetic curves were used in their linear form to obtain the zero-time absorbance by extrapolation. It was assumed that the formation is much more rapid than the disappearance. An iterative procedure has been used to obtain K'. It was considered that at the largest concentration of thiol employed, all Cr(VI) was in the form of the condensed compound. Thus, a first approximation led to a molar absorbance for the complex. With this, for all the other concentrations used, the amount of intermediate was estimated and the equilibrium constant calculated. Using this approximated value of K' one returned to the largest concentration, and computed a corrected value of ε. With this new value the concentration of the intermediate and the equilibrium constant were computed again. The procedure was repeated (8 to 30 iterations) to the convergence of data. The obtained results are presented in table III.6.3.

An alternative way to compute K' and ε is to use the apparent absorption coefficient $\varepsilon_{ap} = A_0/[Cr(VI).\ell$, with ℓ being the path length of the cuvette. From the equilibrium constant the following equation has been derived:

$$\frac{1}{\varepsilon_{ap}} = \frac{1}{K'\cdot\varepsilon}\cdot\frac{1}{[C_6H_5CH_2SH]_0} + \frac{1}{\varepsilon} \qquad 3.6.12$$

From this, a value of K' = 19±2 M^{-1} has been obtained.

Table III.6.3. The initial absorbances at 680 nm in the cell with path lengths of 5 cm, at T = 288 K, [Cr(VI)] = $5.0\cdot10^{-4}$ and computed values of K' and molar absorptivity ε.

10^2 [$C_6H_5CH_2SH$] (M)	A_0	10^5 [$RSCrO_2OAc$] (M)	K' (M^{-1})	ε ($M^{-1}\cdot cm^{-1}$)
1.12	1.545	9.94	22.3	
0.56	0.869	5.67	22.5	3066
0.28	0.437	2.85	21.9	3058
0.224	0.329	2.09	21.9	3142
0.168	0.250	1.56	19.5	3190
		mean:	21.6 ± 3.0	3114 ± 100

Conclusions

The oxidation of α-toluenethiol by Cr(VI) starts with the rapid formation of an intermediate complex in the ratio 1:1 consist with the equilibrium calculation. The steric congestion around the Cr(VI), due to the acetyl group and the bulky benzyl group, hinders the attack of another bulky molecule of the reducing agent in order to directly give the disulfide in a bi-equivalent electron transfer or the disulfide radical anion in a one-equivalent electron transfer. Therefore, a monomolecular decomposition takes place with the implication of new intermediates, Cr(V) and free thiyl radical in the overall course of the reaction. The kinetics, equilibrium and other extra-kinetic data are consistent with the following mechanism

$$C_6H_5\text{-}CH_2SH + HOCrO_2OAc \underset{k_{-1}}{\overset{k_1}{\rightleftharpoons}} C_6H_5\text{-}CH_2SCrO_2OAc + H_2O \qquad 3.6.2$$

$$C_6H_5\text{-}CH_2SCrO_2OAc \longrightarrow C_6H_5\text{-}CH_2S^{\bullet} + Cr^{V}OAc \qquad k_2,\ \textit{e.d.v.} \qquad 3.6.17$$

$$2\ C_6H_5\text{-}CH_2S^{\bullet} \longrightarrow C_6H_5CH_2SS\ CH_2C_6H_5 \qquad 3.6.18$$

$$Cr^{V}OAc + C_6H_5\text{-}CH_2SH_{(excess)} \longrightarrow \text{products} \qquad 3.6.19$$

The more reactive species Cr(V) and free radicals, are consumed as they were formed.

GENERAL CONCLUSIONS

Five redox reaction systems involving three organic compounds in the class of thiols and various oxidizing agents such as Cr(VI), V(V), and $Fe(CN)_6^{3-}$ were scrutinized, concerning their kinetics and mechanisms. There are some common features of these reactions and several differences, especially in the hydrogen-ion intervention.

- All the systems approached exhibit at least two distinguishable steps, which are obvious from their kinetics.
- The first step implies the formation, in a pre-equilibrium, of a long-lived intermediate between the oxidizing species and reducing species by a sulphur link. An exception is hexacyanoferrate(III) which forms an outer-sphere complex instead, because of the inertness to substitution of the Fe(III)-cyano complex.
- These long-lived complexes contain the oxidizing agent in its initial oxidation state and their combination ratio is 1 : 1, with the exception of V(V) where a parallel reaction pathway involves a 2 V(V) to 1 thiol intermediate complex.
- The intermediates were detected directly by spectrophotometry or indirectly from the kinetic rate laws.
- Hydrogen ion intervenes as a catalyst in the complex formation in all Cr(VI) oxidations of the various thiols, whereas with hexacyanoferrate and V(V) as oxidants it has an inhibiting role.

- The decay of these intermediates takes place through electron transfer and obeys first-order kinetics with respect to their concentration.
- The electron-transfer is always the rate determining step. It could involve either one-equivalent or bi-equivalent electron transfer paths, the two being kinetically indistinguishable.
- Generally, the decomposition of the intermediates is assisted by a second thiol molecule, except for the oxidation of α-toluene thiol in acetic acid, where steric effects hinder this involvement.
- The redox process as well can be catalyzed (Cr(VI)) or inhibited by hydrogen ion.

- Under the excess concentration of thiolic compound, the reaction products are always disulfides. This does not exclude the formation of different products when the reactant ratio is inversed.
- ESR or the initiation of polymerization with the redox systems proved the involvement of short-lived free radicals in the overall process.
- The formation of disulfide-ion radical ($RSSR^{-\bullet}$) rather than of the thiyl radical ($RS^{\bullet}$) is considered more probable, albeit the latter being considered in the literature. The arguments for this comes from a stability calculation by MO theory, and the intervention of a second thiol molecule in the electron-transfer process in the case of hexacyanoferrate, a one electron oxidizing agent. Therefore there are no direct proofs to exclude the path of reduction of Cr(VI) to Cr(V) .
- ESR spectroscopy bore witness of the formation of some paramagnetic species, complexes of Cr(V) and V(IV). They behave as relatively long lived intermediates (persist in the reaction mixture for a long time).
- ESR studies also gave evidence to the fact that V(IV) is not the final product of reduction of V(V). Under the excess concentration of reducing agent, the final product is V(III).
- The rate laws deduced from the mechanisms proposed agree well with the experimental ones, providing solid arguments for the proposed reaction networks.

- The employment of the classical method of handling series of pseudo-monomolecular steps in order to determinate rate coefficients for the two processes in the series, using only one kinetic curve with a bi-phasic aspect, might be made with satisfactory results even outside of the condition $k_1 \geq 5k_2$ otherwise stipulated by literature, as demonstrated by our parallel calculations by linear regression and two variants of non-linear regression.

SELECTED REFERENCES

1. M. L. Tobe, *“Inorganic Reaction Mechanisms”*, Nelson and Sons, London, **1972**, Ch. 9.
2. R. G. Wilkins, *“The Study of Kinetics and Mechanism of Reactions of Transition Metal Complexes”*, Allyn and Bacon Inc., Boston, **1974**, Cap. 5, p. 252.
5. H. Taube, H. Meyers, R. L. Rich, “Observations on the mechanism of electron transfer in solution” *J. Am. Chem. Soc.*, **1953**, *75*, 4118-4119.
8. R. A. Marcus, “Chemical and Electrochemical Electron-Transfer Theory”, *Ann. Rev. Phys. Chem.*, **1964**, *15*, 155-196.
10. R. A. Marcus, “Tutorial on rate constants and reorganization energies”*J. Electroanal. Chem.*, **2000**, *483*, 2-6.
13. M. Chou, C. Creutz, N. Sutin, „Rate constants and activation parameters for outer-sphere electron-transfer reactions and comparisons with the predictions of Marcus theory“, *J. Am. Chem. Soc.*, **1977**, *99*, 5615-5623.
14. M. J. Weaver, E. L. Yee, “Activation parameters for homogeneous outer-sphere electron-transfer reactions. Comparisons between self-exchange and cross reactions using Marcus' theory”, *Inorg. Chem.*, **1980**, *19*, 1936-1945.
15. R. D. Cannon, “*Inorganic Reaction Mechanisms”*, **1981**, Ch. 7, p. 3.
16. R. Sarala, S. B. Rabin, D. M. Stanbury, “Oxidation of thiosulfate by tris(phenanthroline) osmium(3+) and related complexes”, *Inorg. Chem.*, **1991**, *30*, 3999-4007.
18. W. R. Fawcett, Yu. I. Kharkats, “Estimation of the free energy of activation for electron transfer reactions involving dipolar reactants and products”, *Electroanal. Chem.*, **1973**, *47*, 413-418.
19. a) B. S. Brunschwig, S. Ehrenson, N. Sutin, “Solvent reorganization in optical and thermal electron-transfer processes“ *J. Phys. Chem.*, **1986**, *90*, 3657-3668; b) B. S. Brunschwig, S. Ehrenson, N. Sutin, „Solvent reorganization in optical and thermal electron-transfer processes: solvatochromism and intramolecular electron-transfer barriers in spheroidal molecules“, *J. Phys. Chem.*, **1987**, *91*, 4714-4719; c) B. S. Brunschwig, N. Sutin, „Energy surfaces, reorganization energies, and coupling elements in electron transfer“, *Coord. Chem. Rev.*, **1999**, *187*, 233-254.
20. a) J. Jortner, I. Rips, M. Weaver, R. W. Fawcett, L. Blum, ”Application of the mean spherical approximation to describe the entropy of solvation of spherical ions in polar solvents”, *J. Chem. Soc. Faraday Trans.*, **1992**, *88*, 3339-3344; b) I. Rips, J. Klafter, J. Jortner, ”Dynamics of ionic solvation”, *J. Chem. Phys.,* **1988**, *88*, 3246-3252; c) I. Rips, J. Klafter, J. Jortner, ” Solvation Dynamics in Polar Liquids”, *J. Chem. Phys.,* **1988**, *89*, 4288-4299.
21. a) G. Grampp, W. Jaenicke, ”ESR spectroscopic investigation of the homogeneous electron-transfer reactions between substituted p-phenylenediamines and quinonediimines, and the validity of Marcus' theory. I. Measurements at 293 K”, *Ber. Bunsenges. Phys. Chem.*, **1984**, *88*, 325-334; b) G. Grampp, W. Jaenicke, ”ESR spectroscopic investigation of the homogeneous electron-transfer reactions between substituted p-phenylenediamines and quinonediimines, and the validity of Marcus' theory. II. Temperature dependence and activation parameters”, *Ber. Bunsenges. Phys. Chem.*, **1984**, *88,* 335-340; c) G. Grampp, W. Jaenicke, ”Kinetics of diabatic and adiabatic electron exchange in organic systems. Comparison of theory and experiment”, *Ber. Bunsenges. Phys. Chem.,* **1991**, *95*, 904-927.
27. G. Grampp, S. Landgraf, **D. Sabou**, D. Dvoranova, **“Application of Marcus cross-relation to mixed inorganic-organic redox couples. A stopped-flow study of the oxidation of N,N,N',N'-tetramethyl-p-phenylenediamine with various oxidants“**, *J. Chem. Soc. Perkin Trans.*, **2002**, *2*, 178-180.
28. N. Sutin, “Electron Transfer in Chemical and Biological Systems”, *Chem. in Britain*, **1972**, 148-151.
29. A. G. Sykes, *“Kinetics of Inorganic Reactions”*, Pergamon Press, Oxford, **1966**, Ch.7.
37. H. Taube, *“Electron Transfer Reactions of Complex Ions in Solution”*, Academic Press, New York, **1970**.
40. E. I. Heiba, R. M. Dessau, W. J. Koehl Jr., „Oxidation by metal salts. V. Cobaltic acetate oxidation of alkylbenzenes“, *J. Am. Chem. Soc.*, **1969,** *91(24)*, 6830-6837.
41. E. I. Heiba, R. M. Dessau, W. J. Koehl Jr., „Oxidation by metal salts. III. Reaction of manganic acetate with aromatic hydrocarbons and the reactivity of the carboxymethyl radical“, *J. Am. Chem. Soc.*, **1969**, *91(1)*, 138-145.
42. K. A. Gardner, L. L. Kuehnert, J. M. Mayer, „Hydrogen Atom Abstraction by Permanganate: Oxidations of Arylalkanes in Organic Solvents“, *Inorg. Chem.*, **1997**, *36*, 2069-2078.
43. L. J. Simmandi, M. Jaky, C. R. Savage, Z. A. Schelly, “Kinetics and mechanism of the permanganate ion oxidation of sulfite in alkaline solutions. The nature of short-lived intermediates”, *J. Am. Chem. Soc.*, **1985**, *107*, 4220-4224.
44. P. George, “The oxidation of ferrous perchlorate by molecular oxygen”, *J. Chem. Soc.*, **1954**, 4349-4359.
45. G. P. Haight, G. M. Jursich, M. T. Kelso, P. J. Merill, “Kinetics and mechanisms of oxidation of lactic acid by chromium(VI) and chromium(V)”, *Inorg. Chem.*, **1985**, *24*, 2740-2746.

46. C. Grant, P. Hambright, “Kinetics of electrophilic substitution reactions involving metal ions in metalloporphyrins”, *J. Am. Chem. Soc.*, **1969,** *91*, 4195-4198.
47. M. D. Cohen, E. Fischer, „Isosbestic points“, *J. Chem. Soc.*, **1962,** 3044-3052.
48. I Bâldea, *“Cinetică chimică şi mecanisme de reacţie. Baze teoretice şi aplicaţii.”*, Presa Universitară Clujeană, **2002**, Ch. 11 and references therein.
56. I. Bâldea, “The reaction between chromate and thiols. IV. The effect of iron(II)-Fe(III) and copper(I)-Cu(II) systems on the oxidation of thioglycolic acid”, *Studia Univ. Babeş-Bolyai, Chem.*, **1989**, *34(1)*, 80-88.
57. P. C. Bulman Page, S. Rosenthal, “A simple and general synthesis of α-keto esters” *Tetrahedron Lett.*, **1986**, *27(17)*, 1947-1950.
58. S. Sattar, K. Kustin, ”Role of osmium în the reacţion of the hydrazinium cation with chlorate în acid soluţion”, *Inorg. Chem.*, **1991**, *30*, 1668-1670.
59. a) E. Erdik, D. S. Matteson, ” Kinetics of osmium tetraoxide catalyzed trimethylamine N-oxide oxidations of cyclohexene and alpha-pinene to diols”, *J. Org. Chem.*, **1989**, *54(11)*, 2742-2748; b) S. W. Kaldor, M. Hammond, “A mild, osmium tetraoxide-catalyzed method for the oxidation of sulfides to sulfones”, *Tetrahedron Lett.*, **1991**, *32(38)*, 5043-5046.
60. S. Ye, F. Han, S. Qu, Y. Wu, “Catalytic action of metal ions în liquid phase oxidation. III. Catalytic action of metal ions especially cerium ion, în the decomposition of tert-butyl hydroperoxide”, *Ranilao Huaxne Xuebao*, **1982**, *10(2)*, 230-237
65. M. Mitewa, P. Bontchev, „Chromium(V) coordination chemistry”, *Coord. Chem Rev.*, **1985**, *61*, 241-272.
66. S. Signorella, S. Garcia, L. Sala, ” Kinetics and mechanism of the oxidation of (±)-2-hydroxy-3-methyl butanoic acid by chromium(VI) in perchloric acid medium”, *Polyhedron*, **1992**, *11*, 1391-1396.
67. S. Ramesh, S. Mahapatro, J. Lui, J. Roček, “Three-electron oxidations. 18. Carbon-13 and deuterium isotope effects in the cooxidation of 2-hydroxy-2-methylbutyric acid and 2-propanol. Evidence for a two-step mechanism”, *J. Am. Chem. Soc.*, **1981**, *103*, 5172-5175.
68. V. Srinivasan, J. Roček, „Three-electron oxidations. 13. Intramolecular cooxidation of 2,7-dihydroxyheptanoic acid. Structure of the transition state in the chromium(VI) oxidation of alcohols“, *J. Am. Chem. Soc.*, **1978**, *100*, 2789-2795.
69. J. F. Perez-Benito, C. Arias, “A kinetic study of the oxidation of L-ascorbic acid by chromium(VI)”, *Int. J. Chem Kinet.*, **1993**, *25*, 221-227.
70. L. Zhang, P. A. Lay, „EPR Spectroscopic Studies of the Reactions of Cr(VI) with l-Ascorbic Acid, l-Dehydroascorbic Acid, and 5,6-O-Isopropylidene-l-ascorbic Acid in Water.1 Implications for Chromium(VI) Genotoxicity”, *J. Am. Chem. Soc.*, **1996**, *118*, 12624-12637.
73. P. H. Connett, K. E. Wetterhahn, „Metabolism of the carcinogen chromate by cellular constituents”, *Struct. Bonding (Berlin.)*, **1983**, *54*, 93-124.
74. P. A. Lay, A. Levina, „Activation of Molecular Oxygen during the Reactions of Chromium(VI/V/IV) with Biological Reductants: Implications for Chromium-Induced Genotoxicities”, *J. Am. Chem. Soc.*, **1998**, *120*, 6704-6714.
75. P. H. Connett, K. E. Wetterhahn, “In vitro reaction of the carcinogen chromate with cellular thiols and carboxylic acids“, *J. Am. Chem. Soc.*, **1985**, *107*, 4282-4288.
76. P. H. Connett, K. E. Wetterhahn, “ Reaction of chromium(VI) with thiols: pH dependence of chromium(VI) thio ester formation“, *J. Am. Chem. Soc.*, **1986**, *108*, 1842-1847.
77. J. F. Perez-Benito, D. Lamrhari, C. Arias, “Three Rate Constants from a Single Kinetic Experiment: Formation, Decomposition, and Reactivity of the Chromium(VI)-Glutathione Thioester Intermediate”, *J. Phys. Chem.*, **1994**, *98*, 12621-12629.
78. P. A. Lay, A. Levina, “Kinetics and Mechanism of Chromium(VI) Reduction to Chromium(III) by l-Cysteine in Neutral Aqueous Solutions”, *Inorg. Chem.*, **1996**, *35*, 7709-7717.
79. J. Darkwa, C. Mundoma, R. H. Simoyi, „Antioxidant chemistry. Reactivity and oxidation of DL-cysteine by some common oxidants”, *J. Chem. Soc., Faraday Trans*, **1998**, *94(14)*, 1971-1978.
80. R. C. Smith, V. D. Reed, T. R. Webb, „Reversal of copper(II)-induced methemoglobin formation by thiols”, *J. Inorg. Biochem.*, **1993**, *52*, 173-182.
81. G. Capozzi, G. Modena, *The chemistry of the thiol group*, in: “*The Chemistry of Functional Groups”*, S. Patai (Ed.), Wiley, New York, **1974**.
99. N. N. Greenwood, A. Earnshaw, *“Chemistry of the Elements”*, 2^{nd} edition, Butterworth-Heinemann, Oxford, UK, 1997.
100. a). H. Taube, “Mechanisms of oxidation-reduction reactions”, *J. Chem. Educ.,* **1968**, *45*, 452-461; b). D. J. Hewkin, R. H. Prince, “The mechanism of octahedral complex formation by labile metal ions “, *Coord. Chem. Rev.*, **1970**, *5*, 45-73.
102. a). A Levina, R. Codd, G. J. Foran, G. J. Hambley, T. W. Maschmeyer, T. Masters, P. A. Lay, „X-ray Absorption Spectroscopic Studies of Chromium(V/IV/III)-2-Ethyl-2-hydroxybutanoato(2-/1-) Complexes”, *Inorg. Chem.*, **2004**, *43*, 1046-1055; b). J. T. Groves, W. J. Kruper Jr., R. C. Haushalter, W. M. Butler, *Inorg. Chem.*, „Synthesis, characterization, and molecular structure of oxo(porphyrinato)chromium(IV)

complexes”, **1982**, *21*, 1363-1368; c). D. J. Liston, B. O. West, „Oxochromium compounds. 2. Reaction of oxygen with chromium(II) and chromium(III) porphyrins and synthesis of a μ-oxo chromium porphyrin derivative”, *Inorg. Chem.*, **1985**, *24*, 1568-1576; d). J. W. Buchler, K. L. Lay, L. Castle, V. Ullrich, „Oxochromium(IV) porphyrins and their relationship to heme proteins”, *Inorg. Chem.*, **1982**, *21*, 842-844; e). L.-C. Yuan, T. C. Bruice, „Mechanism of "oxygen atom" transfer to (tetraphenylporphinato)chromic chloride”, *J. Am. Chem. Soc.*, **1985**, *107*, 512-513.

104. b). M. T. Dickman, M. T. Pope, “Peroxo and superoxo complexes of chromium, molybdenum, and tungsten”, *Chem. Rev.*, **1994**, *94*, 569-584.
105. d). M. C. Ghosh, E. S. Gould, „Electron transfer. 114. Structure-reactivity relationships in the redox series chromium(V,IV,III) and vanadium(V,IV,III)”, *J. Am. Chem. Soc.*, **1993**, *115*, 3167-3173.
108. J. Y. Tong, E. L. King, “A Spectrophotometric Investigation of the Equilibria Existing in Acidic Solutions of Chromium(VI)”, *J. Am. Chem. Soc.*, **1953**, *75*, 6180-6186.
109. G. P. Haight jr., D. C. Richardson, N. H. Coburn, “A Spectrophotometric Study of Equilibria Involving Mononuclear Chromium(VI) Species in Solutions of Various Acids”, *Inorg. Chem.*, **1964**, *3(12)*, 1777-780.
110. b). U. Kläning, M. C. R. Symons, “Structure and reactivity of the oxyanions of transition metals. Part XI. Ultraviolet spectra of monosubstituted chromate ions”, *J. Chem. Soc.,* **1961**, 3204-3208.
111. I. Bâldea, **D. M. Sabou**, **“A comparative study on the oxidation of hydroxy- and mercapto- compounds by Cr(VI)”**, *Studia Univ. Babeş-Bolyai, Chem*, **2001,** *46(1-2),* 17-33.
115. A. McAuley, M. A. Olatunji, “Metal-ion oxidations in solution. Part XIX. Redox pathways in the oxidation of penicillamine and glutathione by chromium(VI)”, *Can. J. Chem.*, **1977**, *55*, 3335-3340.
140. R. P. Farrell, P. A. Lay, A. Levina, I. A. Maxwell, R. Bramley, S. Brumby, J.-Y. Ji, “An EPR Spectroscopic Study of Chromium(V) Oxalato Complexes in Aqueous Solutions. Mechanism of the Chromium(VI) Oxidation of Oxalic Acid”, *Inorg. Chem.*, **1998**, *37*, 3159-3166.
144. S. N. Mahapatro, M. Krumpolc, J. Roček, “Three-electron oxidations. 17. The chromium(VI) and chromium(V) steps in the chromic acid cooxidation of 2-hydroxy-2-methylbutyric acid and 2-propanol”, *J. Am. Chem. Soc.,* **1980**, *102*, 3799-3806.
155. G. Barr-David, M. Charara, R. Codd, R. P. Farell, J. A. Irwin, P. A. Lay, R. Bramley, S. Brumby, J. Y. Ji, G. R. Hanson, “EPR characterisation of the CrV intermediates in the CrVI/V oxidations of organic substrates and of relevance to Cr-induced cancers”, *J. Chem. Soc. Faraday Trans.*, **1995**, *91*, 1207-1216.
156. D. A. Dixon, T. P. Dasgupta, N. P. Sadler, “Mechanism of the oxidation of DL-penicillamine and glutathione by chromium(VI) in aqueous solution”, *J. Chem. Soc., Dalton Trans.*, **1995***(13)*, 2267-2271
172. J. P. McCann, A. McAuley, “Metal-ion oxidations in solution. Part XIII. The reaction of chromium(VI) with L-cysteine in perchlorate media”, *J. Chem. Soc., Dalton Trans.*, **1975**, 783-790.
173. A. McAuley, M. A. Olatunji, “Metal-ion oxidations in solution. Part XVIII. Characterization, rates, and mechanism of formation of the intermediates in the oxidation of thiols by chromium(VI)”, *Can J. Chem.*, **1977**, *55*, 3328-3334.
176. I. Bâldea, “The reaction between chromate and thiols. V. The oxidation of mercaptosuccinic acid”, *Studia Univ. Babeş-Bolyai, Chem.*, **1994**, *39(1-2),* 138-149.
177. I. Bâldea, “The reaction between chromate and thiols. III. The oxidation of thioglycolic acid“, *Studia Univ. Babeş-Bolyai, Chem.*, **1987**, *32(2),* 42-49.
179. I. Bâldea, G. Niac, “The reaction between chromate and thiols. II. The oxidation of cysteine”, *Studia Univ. Babeş-Bolyai, Chem.*, **1986**, *31(2),* 41-48.
180. I. Bâldea, G. Niac, “Reaction between chromate and thiosulfate. II. Kinetics of tetrathionate formation”, *Inorg. Chem.*, **1970**, *9*, 110-114.
181. J. F. Perez-Benito, C. Arias, D. Lamrhari, “The determination of kinetic data for the reactions of chromium(VI) with glutathione and other thiols”, *Int. J. Chem. Kinet.*, **1994**, *26*, 587-591.
183. G. Niac, S. Schön, I. Bâldea, “The reaction between chromate and thiols. I. The oxidation of ethanethiol “, *Studia Univ. Babeş-Bolyai, Chem.*, **1986**, *31(2)*, 31-40.
184. Z. M. Hoffman, E. Hayon, „One-electron reduction of the disulfide linkage in aqueous solution. Formation, protonation, and decay kinetics of the RSSR- radical“, *J. Am. Chem. Soc.*, **1972**, *94(23)*, 7950-7957.
185. M. T. Pope, B. W. Dale, “Isopolyvanadates, -niobates, and –tantalates”, *Quart. Rev. Chem. Soc.*, **1968**, *22*, 527-548
186. M. T. Pope, *„Heteropoly and Isopoly Oxometalates”,* Springer Verlag, Berlin, Heidelberg, New York, Tokio, **1983**, pp.34-38 şi referinţele incluse.
195. a) B. W. Clare, D. L. Kepert, D. W. Watts, “Kinetic study of the acid decomposition of decavanadate”, *J. Chem. Soc. Dalton Trans.*, **1973**, 2479-2480; b) B. W. Clare, D. L. Kepert, D. W. Watts, “Acid decomposition of decavanadate: specific salt effects”, *J. Chem. Soc. Dalton Trans.*, **1973**, 2481-2487
214. E. E. Kriss, K. B. Yatsimirskii, G. T. Kurbatova, A. S. Grigor’eva, “Reduction of vanadate by ascorbic acid studied by an EPR method”, *Russ. J. Inorg. Chem.*, **1975**, *20(1)*, 101-107
215. E. E. Kriss, G. T. Kurbatova, K. B. Yatsimirskii, ” Kinetics of the reduction of polyvanadate by ascorbic acid studied by an EPR method”, *Russ. J. Inorg. Chem.*, **1975**, *20*, 108-111.

216. W. F. Pickering, A. McAuley, “Metal-ion oxidations in solution. Part III. The oxidation of 2-mercaptosuccinic acid by vanadium(V)”, *J. Chem. Soc.* (A), **1968**, 1173-1176

217. A. McAuley, “The role of complexes in metal-ion oxidations in solution”, *Coord. Chem. Rev.*, **1970**, *5*, 245-273

218. A. J. Tasiopoulos, A. N. Troganis, A. Evangelou, C. P. Raptopoulou, A. Terzis, Y. Deligiannakis, T. A. Kabanos, “Synthetic Analogues for Oxovanadium(IV)–Glutathione Interaction: An EPR, Synthetic and Structural Study of Oxovanadium(IV) Compounds with Sulfhydryl-Containing Pseudopeptides and Dipeptides”, *Chem. Eur. J.*, **1999**, *5(3),* 910-921

219. M. T. Armas, A. Mederos, P. Gili, S. Dominguez, R. Hernandez-Molina, P. Lorenzo, E. J. Baran, M. L. Araujo, F. Brito, “Speciation in the oxovanadium(IV)/glutathione system”, *Polyhedron*, **2001**, *20*, 799-804

221. P. L. Domingo, B. García, J. M. Leal, „Acid–base behaviour of the ferricyanide ion in perchloric acid media. Spectrophotometric and kinetic study”, *Can. J. Chem.*, **1990**, *68*, 228-235.

225. J. M. Leal, B. García, P. L. Domingo, “Outer-sphere Hexacyanoferrate(III) Oxidation of Organic Substrates”, *Coord. Chem. Rev.*, **1998**, *173*, 79-131.

227. P. L. Domingo, B. García, J. M. Leal, „Acid–base behaviour of the ferrocyanide ion in perchloric acid media potentiometric and spectrophotometric study”, *Can. J. Chem.*, **1987**, *65*, 583-589.

233. A. Messina, G. Gritzner, „Polarographic and voltammetric studies of tetrabutylammonium hexacyanoferrate(III) and tetrabutylammonium hexacyanomanganate(III) in non-aqueous “, *J. Electroanal. Chem.*, **1979**, *101*, 201-209.

234. V. Gutmann, G. Gritzner, K. Danksagmüller, „Solvent effects on the redox potential of hexacyanoferrate(III)-Hexacyanoferrate(II)”, *Inorg. Chim. Acta*, **1976**, *17*, 81-86.

298. a) **D.-M. Sabou**, I Bâldea, **“Cinetica reactiei de oxidare a acidului tiolactic cu Cr(VI) in mediu acid”**, *A XXVII-a Conferinta Nationala de Chimie*, 23 - 25 octombrie **2002**, Calimaneşti-Caciulata. (poster); b) **D.-M. Sabou**, I. Bâldea, **“Cinetica si mecanismul oxidării acidului tiolactic cu Cr(VI) şi $Fe(CN)_6^{3-}$. Studiu comparativ.”**, *Conferinta Nationala de Chimie*, 7 - 9 mai **2003**, Baia Mare. **(oral communication)**; c) **D.-M. Sabou**, I. Bâldea, **“A Comparative Kinetic Study on the Thiolactic Acid Oxidation by Cr(VI), V(V) and $Fe(CN)_6^{3-}$ in Acidic Medium”**, *11th Physical Chemistry Conference (ROMPHYSCHEM 11)*, 2 - 5 septembrie **2003**, Timişoara. (poster); d) **D.-M. Sabou**, I Bâldea, **“On the Kinetics of Thiolactic Acid Oxidation by Cr(VI), V(V) and $Fe(Cn)_6^{3-}$ in Acidic Media”**, *A XIII-a Conferinta Internationala de Chimie si Inginerie Chimica*, 13 - 15 septembrie **2003**, Bucureşti. (poster)

299. a). R. N. Bose, S. Moghaddas, E. Gelerinter, „Long-lived chromium(IV) and chromium(V) metabolites in the chromium(VI)-glutathione reaction: NMR, ESR, HPLC, and kinetic characterization” *Inorg. Chem*, **1992**, 31(11), 1987-1994; b). S. Moghaddas, E. Gelerinter, R. N. Bose, „Mechanisms of formation and decomposition of hypervalent chromium metabolites in the glutathione-chromium(VI) reaction” *J. Inorg. Biochem.*, **1995**, 57, 135-146.

300. T. Carrington, „Estimation of rate constants from growth and decay data” *Int. J. Chem. Kinet.*, **1982**, *14(5)*, 517-534.

301. a) I. Bâldea, **D.-M. Sabou**, A. Csavdari, **“One-Plus Rate Equation, an Useful Tool to Elucidate the Reaction Mechanism”**, *Studia Universitatis Babeş-Bolyai, Ser. Chem.*, **2007**, *52(1),* 19-34; b) A. Csavdari, I. Bâldea, **D.-M. Sabou**, **“Oxidation of DL-Methionine (2-Amino-4-ethylthiobutanoic Acid) by Chromate. Mechanistic Interpretation on the Base of an One-Plus Rate Equation”**, *Studia Universitatis Babeş-Bolyai, Ser. Chem.*, **2007**, *52(3),* 113-120.

302. a) J. H. Espenson, „Oxidation of transition metal complexes by chromium (VI)” *Accounts Chem. Rev.* **1970**, *3*, 347-353; b). A. Levina, L. Zhang, P. A. Lay, “Structure and Reactivity of a Chromium(V) Glutathione Complex” *Inorg. Chem.* **2003**, *42(3)*, 767-784.

303. **D.-M. Sabou,** I. Bâldea, **„Kinetics of thiolactic acid oxidation by decavanadate and VO_2^+ in acidic media”**, *Studia Univ. Babeş-Bolyai, Ser. Chem.*, **2004**, *49(1),* 55-64.

304. Ioan Bâldea, **Dana-Maria Sabou**, Alexandra Csavdari **„Oxidation of 2-mercaptopropionic acid by hexacyanoferrate-(III). Mechanistic interpretation on the basis of one-plus rate equation.”** *Revue Roumaine de Chimie,* **2009**, *5*4(10), 791–798.

305. a) I. Bâldea, **D. M. Sabou**, **„The Kinetic Study on the Oxidation of Glutathione by Cr(VI) in Acidic Media”**, *A 12-a Conferinta Internationala de Chimie şi Inginerie Chimica din Romania*, Universitatea Politehnica Bucureşti, Facultatea de Chimie Industriala, 13 - 15 septembrie **2001**. (poster); b) **D.-M. Sabou**, I Baldea, **“Glutahione Oxidation by Chromate in Acidic Medium. Kinetic Aspects and some Reaction Intermediates.”**, *Conferinta internationala “Several aspects of Biology, Chemistry, Informatics, Mathematics and Physics”*, 11-13 noiembrie **2005**, Oradea. (poster)

306. I. Bâldea, **D.-M. Sabou**, **„The reaction between chromate and thiols. VI. The oxidation of benzenethiol and α-toluenethiol in acetic acid solutions”**, *Rev. Roum. Chim.*, **2000**, 45(6), 537-544.